



HAL
open science

U–Pb detrital zircon dates and source provenance analysis of Phanerozoic sequences of the Congo Basin, central Gondwana

Bastien Linol, Maarten J. de Wit, Erika Barton, Michiel C.J. de Wit, François Guillocheau

► To cite this version:

Bastien Linol, Maarten J. de Wit, Erika Barton, Michiel C.J. de Wit, François Guillocheau. U–Pb detrital zircon dates and source provenance analysis of Phanerozoic sequences of the Congo Basin, central Gondwana. *Gondwana Research*, 2016, 29 (1), pp.208-219. 10.1016/j.gr.2014.11.009 . insu-01120212

HAL Id: insu-01120212

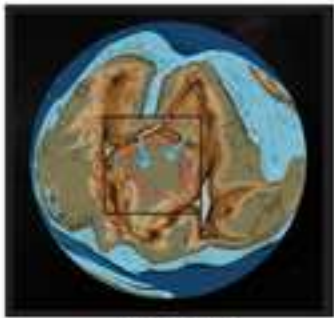
<https://insu.hal.science/insu-01120212>

Submitted on 25 Feb 2015

HAL is a multi-disciplinary open access archive for the deposit and dissemination of scientific research documents, whether they are published or not. The documents may come from teaching and research institutions in France or abroad, or from public or private research centers.

L'archive ouverte pluridisciplinaire **HAL**, est destinée au dépôt et à la diffusion de documents scientifiques de niveau recherche, publiés ou non, émanant des établissements d'enseignement et de recherche français ou étrangers, des laboratoires publics ou privés.

A) Late Neoproterozoic to early Paleozoic



550-450 Ma

B) Carboniferous to Permian



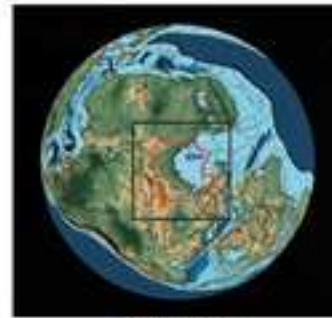
350-300 Ma

C) Triassic



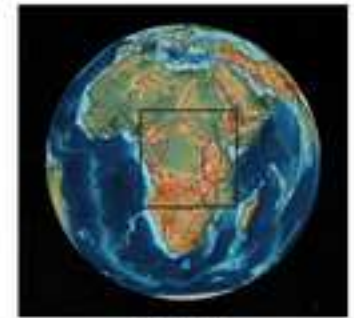
250-200 Ma

D) Late Jurassic to Early Cretaceous



150-100 Ma

E) Mid-Cretaceous to Cenozoic



100-0 Ma



*Highlights (for review)

- A revised stratigraphy for one of the least-known large continental basins
- Track the evolution of central Gondwana via U-Pb detrital zircon geochronology
- Early Neoproterozoic (1 Ga) dates dominated in all samples

U-Pb detrital zircons dates and source provenance analysis of Phanerozoic sequences of the Congo Basin, central Gondwana

Bastien Linol^{1,2}, Maarten J. de Wit¹, Erika Barton^{1,2}, Michiel (Mike) J.C. de Wit³ and Francois Guillocheau⁴

¹ AEON-ESSRI (African Earth Observatory Network – Earth Stewardship Science Research Institute.

² Department of Geoscience, Nelson Mandela Metropolitan University, Port Elizabeth, South Africa.

Corresponding author: bastien.aeon@gmail.com

³ Delrand Resources Pty Ltd., Toronto, Ontario, Canada.

⁴ Geosciences, University of Rennes1, France.

Abstract

The Congo Basin (CB) is the largest sediment sink of central Gondwana, built on a mosaic of Precambrian crustal blocks amalgamated during the mid-Paleoproterozoic (Eburnian; 2.1-1.8 Ga), late Mesoproterozoic (Kibaran; 1.4-1.0 Ga), and late Neoproterozoic-early Cambrian (Pan African; 750-500 Ma). Sporadic uplift, tilting and erosion of these Precambrian terrains form the source regions for the sedimentary sequences that fill the CB. We investigate the Phanerozoic successions in the field and along four historic deep boreholes drilled in the center of the basin, and date detrital zircons from the main stratigraphic groups to characterize their provenance ages and reconstruct the paleogeographic evolution of the CB during amalgamation and break-up of the Gondwana supercontinent. Sedimentological data show that the oldest, upper Neoproterozoic-lower Paleozoic Redbeds (the Inkisi, Aruwimi and Bianco Groups) were derived from the north. Zircons from these sequences have two dominant age-populations of 1100-950 Ma and 800-600 Ma, likely sourced from Kibaran and Pan African terrains within the Oubanguides (e.g. the Central Saharan Belt) and parts of the North African Shield (e.g. Darfour). The overlying Carboniferous-Permian glacial and deglaciation sequences (the Lukuga Group) have similar peaks, as well as abundant zircons of 2.05-1.85 Ga and a subordinate number dated at 1.42-1.37 Ga. The latter are from Eburnian and Kibaran sources in east-central Africa, consistent with west-facing glacial paleo-valleys preserved along the

1 eastern margin of the CB. The succeeding Triassic (the Haute-Lueki Group) and
2 Jurassic-Cretaceous (the Kwango Group) fluvial and aeolian red sandstones were
3 again derived from the north. Their range of zircon dates also has two main peaks at
4 1000 Ma and 600 Ma, but also contain small younger grains of 290-240 Ma and 200-
5 190 Ma. We interpret these younger zircons to be derived from volcanic dust that
6 originated during late Paleozoic-Jurassic magmatism of the Choiyoi and Chon Aike
7 Provinces flanking the Andean subduction margin of Gondwana. By contrast, the
8 uppermost Cenozoic alluviums of the CB (the Kalahari Group) contain diamond
9 concentrates and large zircon fragments dated at 3-2.5 Ga, derived from the Kasai and
10 Cuango Cratons, to the south, which host Cretaceous diamondiferous kimberlites.
11
12
13
14
15
16
17
18
19

20 Keywords: Phanerozoic, Congo Basin, detrital zircons, sediment provenances, central
21 Gondwana.
22
23
24
25

26 **1. Introduction**

27
28

29 The Congo Basin (CB) is a large (ca. 1.8 million km²) Phanerozoic sedimentary basin
30 near the center of Africa (Fig. 1) whose origin and tectonic evolution are poorly
31 understood, mostly because of a lack of modern chronostratigraphy (Kadima et al.,
32 2011; Sachse et al., 2012; Linol, 2013; Linol et al., 2014a, and b; de Wit and Linol,
33 2014). The CB was initially explored during the 1940s and 1950s, when that region,
34 now the Democratic Republic of Congo (DRC), was part of the Belgian Congo. This
35 early work included extensive field mapping (e.g. Robert, 1946; Cahen, 1954;
36 Lepersonne, 1974), geophysical surveys (e.g. Jones et al., 1959; Evrard, 1960), and
37 the drilling and coring of two deep boreholes (each ca. 2 km deep), named Samba and
38 Dekese (Cahen et al., 1959, and 1960). These holes represent unique stratigraphic
39 sections through the center of the basin and are now archived at the Royal Museum
40 for Central Africa (RMCA) in Tervuren (Belgium). In the 1970s, after independence,
41 petroleum exploration companies acquired new seismic reflection data along 36
42 profiles, and drilled two more (non-cored) deep boreholes, the Gilson-1 and
43 Mbandaka-1 wells (each more than 4 km deep; EssoZaire, 1981a, and b; Lawrence
44 and Makazu, 1988; Daly et al., 1991, and 1992). This data was used to define the
45 geometry of main stratigraphic sequences and revealed in subsurface a series of
46 northwest-southeast trending basement highs near the center of the basin. These highs
47
48
49
50
51
52
53
54
55
56
57
58
59
60
61
62
63
64
65

1 were interpreted to have formed as a result of far-field tectonic stresses during
2 Neoproterozoic and late Paleozoic collision processes along Gondwana's paleo-
3 Pacific margins (Daly et al., 1991, and 1992; Trouw and de Wit, 1999). Since these
4 two exploration programs, very little new stratigraphic data has been acquired across
5 the CB, hampering regional correlations and modern interpretation of its geodynamic
6 history (Giresse, 2005; Crosby et al., 2010; Kadima et al., 2011; Buiter et al., 2012;
7 Linol et al., 2014c).

8
9 Here, we present new U-Pb detrital zircon dates from outcrops along the Kwango
10 River in southwestern DRC, and from selected core samples of the Samba and Dekese
11 sections. Together with improved field, seismic and borehole stratigraphic
12 correlations, sediment dispersal directions, and a review of dated basement rocks in
13 and around central Africa (and central Gondwana), this source provenance analysis
14 attempts to retrace the paleogeographic evolution of the CB during the Phanerozoic,
15 from the time of final assembly to the break-up of the Gondwana supercontinent.
16 Although the regional extent (one field study and two boreholes sites) and number of
17 samples (9 samples) are limited, these U-Pb results are among the first detrital zircon
18 dates for the CB, providing new information on the geodynamic history of interior
19 Gondwana.
20
21
22
23
24
25
26
27
28
29
30
31
32
33
34
35

36 **2. Geological setting**

37 The CB is completely surrounded by Precambrian rocks, including several Archean
38 cratonic blocks (i.e. cratons) and Proterozoic belts with regionally distinct geologic
39 and thermo-tectonic histories, together referred to as the Central African Shield (de
40 Wit et al., 2008; de Wit and Linol, 2014; Fig. 1A). This shield amalgamated with
41 others continental fragments (e.g. the Kalahari and North African Shields) during the
42 late Neoproterozoic to early Cambrian Pan African orogens (750-500 Ma; Fritz et al.,
43 2013) to form central Gondwana, thereafter making up the foundation (i.e. crystalline
44 basement) and providing sediments to the Phanerozoic CB (Fig. 1B).
45
46
47
48
49
50
51
52

53 [Figure 1 here]

54 **Precambrian basement**

55 The Central African Shield comprises the Kasai, NE Angola (Cuango), Ntem,
56 Mboumou and Tanzanian Cratons (ca. 3.5-2.5 Ga; Cahen et al., 1984), surrounding
57
58
59
60
61
62
63
64
65

1 the CB (Fig. 1A). These blocks amalgamated with mid-Paleoproterozoic terrains
2 along the Ruwenzori and Ubendian-Usagaran Belts (ca. 2.1-1.8 Ga) in Uganda and
3 western Tanzania (Lenoir et al., 1995; Link et al., 2010; Boniface et al., 2012), the
4 Central Angolan Mobile Belt (CAMB; ca. 2.3-2.0 Ga) in Angola (de Carvalho et al.,
5 2000; de Wit and Linol, 2014), and the West Central African Mobile Belt (WCAMB;
6 ca. 2.5-2.0 Ga) in western DRC, Gabon and Cameroon (Caen-Vachette et al., 1988;
7 Feybesse et al., 1998), that extends to Transamazonian terrains in northeastern Brazil
8 (e.g. Toteu et al., 2001; Lerouge et al., 2006; Pedrosa-Soares et al., 2008). This
9 assemblage was subsequently affected by mid-Mesoproterozoic granitoid magmatism
10 along the Kibaran Belt in eastern DRC, Rwanda and Burundi (ca. 1.4 Ga; Tack et al.,
11 2010; Fernandez-Alonso et al., 2012), and again deformed during the late
12 Mesoproterozoic to early Neoproterozoic (ca. 1 Ga) within the Oubanguides in the
13 Central African Republic (CAR) and Chad (e.g. the Central Saharan Belt; de Wit et
14 al., 2014), and along the Irumide-Mozambique Belts in Zambia and northern
15 Mozambique (Jamal, 2005; de Waele et al., 2008; Bingen et al., 2009; Roberts et al.,
16 2012).

17
18
19
20
21
22
23
24
25
26
27
28
29 A Central African Shield was then finally consolidated during the Pan African along a
30 vast system of peripheral mobile belts, folded-and-thrusted concentrically toward the
31 proto-CB. This includes: the ca. 700-500 Ma West Congo Belt (de Carvalho et al.,
32 2000; Tack et al., 2001; Frimmel et al., 2006; Monié et al., 2012); the Oubanguides
33 (ca. 850-550 Ma; Poidevin, 1985; Rolin, 1995; Toteu et al., 2006; Nkoumbou et al.,
34 2013); the Mozambique Belt (ca. 700-550 Ma; Sommer et al., 2003; de Waele et al.,
35 2006; Fritz et al., 2013); and the Lufilian Arc (ca. 750-550 Ma; Kampunzu and
36 Cailteux, 1999) in southeastern DRC and northern Zambia that extends to the
37 southwest in northern Botswana and Namibia (de Wit, 2009; Rankin et al., 2013). All
38 these Pan African mobile belts link to a northeast- and southwest-verging thrust, or
39 “flower structure” (the Kiri High; Daly et al., 1991, and 1992), inferred to exist
40 beneath the center of the CB (Fig. 1A).

41 42 **Phanerozoic cover of the Central African Shield**

43
44
45
46
47
48
49
50
51
52
53
54
55
56
57
58
59
60
61
62
63
64
65
The CB preserves five main depositional successions (or “supersequences”; Linol,
2013, see also Linol et al., 2014d) ranging in age from late Neoproterozoic to
Cenozoic, with a total thickness of 4-6 km near the center of the basin (Fig. 2).

[Figure 2 here]

1 The oldest succession, uppermost part of the Neoproterozoic to lower Paleozoic West
2 Congo, Lindi and Katanga Supergroups (Lepersonne, 1974; Poidevin, 1985; Tack et
3 al., 2001; Kanda et al., 2011; Tait et al., 2011), comprises about 1-1.5 km thick
4 Redbeds, deposited regionally southward unconformably across deformed
5 Precambrian carbonate and siliclastic platforms that are exposed around the margins
6 of the CB (Fig. 1B). This includes: the Aruwimi Group that outcrops abundantly
7 south of the Oubanguides; the Inkisi Group, east of the West Congo Belt (Alvarez et
8 al., 1995); and the Bianco Group to the north of the Lufilian Arc (Master et al., 2005).
9 Their stratigraphy is relatively poorly constrained by field observations and
10 geochronology, and only detrital zircons dated at 540 Ma provide a maximum early
11 Cambrian age (Jelsma et al., 2011). Equivalent subsurface sequences of red quartzites
12 have been proven only in the Gilson-1 and Dekese wells (Units G10 and D10; Fig. 2)
13 in the south-central part of the basin.
14
15
16
17
18
19
20
21
22

23 A major erosion surface across the Redbeds represents a hiatus of up to 150 million
24 years. This unconformity is overlain by Carboniferous-Permian and Triassic
25 successions, in total between 1 km and 3 km thick, which represent the northern
26 extensions of the Karoo Supergroup of southern Africa (e.g. Johnson et al., 1996;
27 Catuneanu et al., 2005; Linol et al., 2014a). The lowermost parts, the Lukuga Group,
28 are glacial and deglaciation sequences of diamictite and black shale, and sandstones
29 with thin coal beds, dated by paleobotany from mid-Carboniferous to Late Permian
30 (Boulouard and Calandra, 1963; Bose and Kar, 1978; Colin and Jan du Chêne, 1981).
31 The Lukuga Group is best preserved in east-west-trending paleo-valleys along the
32 eastern margin of the CB (Jamotte, 1932; Boutakoff, 1948; Cahen and Lepersonne,
33 1978; Fig. 1B), and extends in subsurface to the south-central and western parts of the
34 basin (ca. 900 m thick at Dekese; Fig. 2). The overlying Triassic Haute Lueki Group
35 is less precisely described in outcrop (Lombard, 1961; Bose and Kar 1976; Cahen,
36 1981) but, most likely is laterally equivalent to widespread arid fluvial-aeolian
37 sequences (also “red-beds”) in south-central Africa, such as for example the Cassange
38 Group in Angola (Antunes et al., 1990), the Lebung Group in Botswana (Bordy et al.,
39 2010), the Omingonde Formation in Namibia (Miller, 2008), the Beaufort and
40 Stormberg Groups in South Africa (Johnson et al., 1996; Tankard et al., 2012), and in
41 eastern Brazil (e.g. the Santa Maria Group; Zerfass et al., 2004; Milani et al., 2007). It
42 is between 500 m and 1800 m thick in the center of the CB (ca. 900 m at Samba; Fig.
43 2).
44
45
46
47
48
49
50
51
52
53
54
55
56
57
58
59
60
61
62
63
64
65

1
2
3
4
5
6
7
8
9
10
11
12
13
14
15
16
17
18
19
20
21
22
23
24
25
26
27
28
29
30
31
32
33
34
35
36
37
38
39
40
41
42
43
44
45
46
47
48
49
50
51
52
53
54
55
56
57
58
59
60
61
62
63
64
65

Above these sequences, and overlying a pronounced unconformity that coincides in time with the onset of break-up of Gondwana (ca. 200-160 Ma; Reeves, 1999; Jokat et al., 2003; Torsvik et al., 2012), are Upper Jurassic to Upper Cretaceous sequences of red sandstones, between 500 m and 1000 m thick, which cover the entire CB (Fig. 1B). At the base, the fluvial-deltaic Stanleyville Group intercalates in its lower part with a fossiliferous marine limestone horizon (“Lime Fine”; Cahen, 1983a) that implies a short Kimmeridgian transgression of the proto-Indian Ocean in the northeastern CB (Saint-Seine, 1955; Saint-Seine and Casier, 1962; Taverne, 1975; Giresse, 2005; Linol, 2014b). It is overlapped to the south by northeasterly-derived aeolian dunes of the Lower Kwango Group (Units D4 and G4; Fig. 2), extending continuously to the southwestern margin of the basin (Fig. 3A), and into the Paraná Basin of eastern Brazil (see Linol, 2013, and Linol et al., 2014d for details). In the center of the CB, the succeeding Loia and Bokungu Groups correspond to two superimposed lacustrine sequences (in total ca. 650 m thick at Samba; Fig. 2), both dated biostratigraphically to be Albian-Cenomanian in age (Marlière, 1950; Cox, 1960; Defrétin-Lefranc, 1967; Grékoff, 1957; Maheshwari et al., 1977; Colin, 1981; Cahen, 1983b). These sequences are overlain in the west-central part of the basin by Upper Cretaceous (also fossiliferous) fluvial red sandstones and mudstones of the Upper Kwango Group (Lepersonne, 1951; Saint Seine 1953; Grékoff, 1960; Casier, 1965; Taverne, 1976; Colin, 1994; Linol et al., 2014b).

[Figure 3 here]

The Jurassic-Cretaceous succession of the CB is in turn truncated by a peneplanation surface, covered by silcretes (“Polymorph Sandstones”; c.f. Lepersonne 1951) and alluviums of the Cenozoic Kalahari Group (Leriche, 1927; Polinard, 1932; Grékoff, 1958; de Ploey et al., 1968; Colin, 1994; e.g. Fig. 3B). This youngest sequence is between 40 m and 240 m thick in the center of the basin (Fig. 2).

3. Material and methods

Detrital zircons from nine samples, collected in the field (Fig. 3) and from the Samba and Dekese cores (Fig. 2), were U-Pb dated by Laser Ablation Multi-Collector Inductively Coupled Plasma Mass Spectrometry (LA-MC-ICP-MS; e.g. Cocherie and Robert, 2008). Together with the new sequence-stratigraphic correlations and sediment dispersal directions described above, this geochronology helps

1 understanding the evolution of source provenance ages and associated major
2 geological changes during development of the Phanerozoic CB (e.g. Fedo et al.,
3 2003).
4
5

6 **Core samples and preparation**

7
8 Sampling was done during fieldwork in the Kwango region of the southwest CB, and
9 while logging the Samba and Dekese sections archived at the Royal Museum for
10 Central Africa (RMCA) in Tervuren (Belgium). Two samples from outcrops and
11 seven samples from the two core-sections were analyzed (Figs. 2 and 3), representing
12 10 kg and 50 kg of red sandstones and gravels, and between 1 m and 5 m of bisected
13 core (1.5-3.5 kg each), respectively.
14
15

16
17 Heavy minerals were concentrated in the field using an Armstrong-Jig, and in
18 laboratory with the application of heavy liquid (Lithium-based Tungstate) and a
19 Frantz isodynamic separator, at the University of Cape Town (South Africa) and the
20 University of Heidelberg (Germany). The concentrates were examined under the
21 binocular microscope and for each sample between 150 and 200 zircons with different
22 size, shape, color and abundance were carefully hand-picked. Selected grains (e.g.
23 Fig. 4) were then mounted into epoxy disks, abraded down to the center of grains and
24 polished. The mounts were imaged using a JEOL microprobe in both
25 cathodoluminescence and backscatter electron modes to further characterize the
26 internal composition and structure of the zircons (e.g. zoning, inherited cores,
27 overgrowths, recrystallization and fractures). These images are also used to guide the
28 laser to specific sites during U-Pb dating (e.g. Fig. 5).
29
30
31
32
33
34
35
36
37
38
39
40

41 [Figure 4 here]
42
43

44 **Analytical method of dating**

45 U-Pb dating was performed in the AEON EarthLab, using a Nu Plasma HR multi-
46 collector inductively coupled plasma mass spectrometer (Nu Instruments) coupled to
47 a UP 193 solid-state laser system (New Wave Research) and a desolvation nebulizer
48 system (DSN-100, Nu Instruments). The Nu Plasma MC-ICP-MS is equipped with a
49 special collector block allowing for simultaneous detection of ion signals from masses
50 ^{238}U to ^{203}Tl . U and Tl isotopes are measured on Faraday cups, while Pb isotopes are
51 measured on ion counters. For more details see Biggin et al. (2011), and for the
52 general analytical routine Simonetti et al. (2005).
53
54
55
56
57
58
59
60
61
62
63
64
65

1 U and Pb data was collected in time-resolved mode including 20 s of instrument
2 background, 20 s of gas and acid blank, and 35 s of sample ablation. The laser was
3 operated at a repetition rate of 10 Hz and an energy density of 2-3 J/cm². The spot
4 size varied from 15 μm to 35 μm depending on the size and on the Pb concentration
5 of the analyzed zircon. Raw data were corrected from background signals. Mass bias
6 correction of the ²⁰⁷Pb/²⁰⁶Pb ratio was done using the Tl-doping method of Belshaw et
7 al. (1998). Laser-induced inter-element fractionation and time-dependent Pb/U
8 fractionation of the ²⁰⁶Pb/²³⁸U ratio was corrected by standard bracketing of 10
9 unknowns, with the reference material represented by a fragment of the 611 Ma GJ1
10 zircon standard with an U concentration of ~ 450 ppm. ²⁰⁷Pb/²³⁵U was calculated
11 using $^{207}\text{Pb}/^{235}\text{U} = ^{207}\text{Pb}/^{206}\text{Pb} \times ^{206}\text{Pb}/^{238}\text{U} \times 137.88$. Reported uncertainties were
12 propagated by quadratic addition of the external reproducibility of the standard during
13 the individual analytical session and the internal error of the respective analysis.
14 Reported dates in this study are not common Pb corrected, since correction by the
15 ²⁰⁴Pb method cannot be applied due to the isobaric interference of ²⁰⁴Hg, which is a
16 contaminant of the He gas carrying the ablated material from the laser cell to the MC-
17 ICP-MS. The accuracy of the data was checked by regular analyses of internal
18 standards: from the Kaap Valley pluton (3227 ± 1 Ma; Kamo and Davis, 1994), and
19 the Plešovice zircon standard (337.13 ± 0.37 Ma; Sláma et al., 2008). Concordia plots
20 and probability diagrams were constructed using Isoplot 3.0 (Ludwig, 2003).

38 4. Results

39 In total, 568 detrital zircons were analyzed from the different stratigraphic groups
40 (Fig. 5). The U-Pb data for each sample (between 60 and 80 analyses) are presented in
41 Tables 1 to 9. Below, we discuss only ²⁰⁶Pb/²⁰⁷Pb dates that are concordant in the
42 range of 90-110%, unless otherwise mentioned (for the grains younger than 500 Ma).

43 [Figure 5 here]

44 [Tables 1 to 9 about here]

52 Sample D1853 (the Inkisi Group)

53 63 analyses were performed on 60 grains in samples D1853 (Table 1) from red
54 quartzitic sandstones of the Inkisi Group in the lower part of the Dekese section (Fig.
55 2). Zircons from this sample are relatively small, sub-rounded and brownish in color
56 (Fig. 4A).

1
2
3
4
5
6
7
8
9
10
11
12
13
14
15
16
17
18
19
20
21
22
23
24
25
26
27
28
29
30
31
32
33
34
35
36
37
38
39
40
41
42
43
44
45
46
47
48
49
50
51
52
53
54
55
56
57
58
59
60
61
62
63
64
65

42 single zircon dates are concordant (in the range of 90-110%). The four oldest date between 2671 ± 5 Ma and 2575 ± 9 Ma. Two zircons date at 2.0 Ga (2041 ± 7 Ma and 2036 ± 10 Ma), 22 date between 1107 ± 12 Ma and 881 ± 20 Ma (52%) that represent the most abundant age-population, and 14 date between 835 ± 8 Ma and 609 ± 21 Ma (33%). Following this distribution, the probability plot shows peaks at 2670 Ma, 2060 Ma, 1040 Ma and 650 Ma (Fig. 5A).

Samples D1400 and D1595 (the Lukuga Group)

In samples D1400 and D1595, from diamictites of the Lukuga Group in the middle part of the Dekese section (Fig. 2), 157 analyses were performed on 148 grains (Tables 2 and 3). Zircons from this group are small to large (200-500 μ m), sub-rounded and generally transparent (Fig. 4B).

In total 123 single zircon dates are concordant. The oldest zircon dates at 2925 ± 8 Ma. Six zircons date between 2690 ± 16 Ma and 2428 ± 16 Ma, one dates at 2.2 Ga (2184 ± 16 Ma), and 41 date between 2074 ± 20 Ma and 1802 ± 12 Ma (31%) that represent the most abundant age-population in the samples. Seven zircons date between 1589 ± 28 Ma and 1371 ± 18 Ma, 40 are between 1235 ± 9 Ma and 964 ± 20 Ma (30%), and 27 date between 865 ± 25 Ma and 544 ± 21 Ma (20%). The probability plot shows three distinct peaks at 1930 Ma, 1040 Ma and 680 Ma (Fig. 5B).

Samples S1605 and S2035 (the Haute Lueki Group)

In samples S1605 and S2035, from red quartzitic sandstones of the Haute Lueki Group in the lower part of the Samba section (Fig. 2), 124 analyses were performed on 105 grains (Tables 4 and 5). Zircons from these samples are relatively small, elongated and transparent or brownish in color (Fig. 4C); some have xenotime overgrowths.

In total 56 single zircon dates are concordant. Many zircons are systematically discordant due to common lead loss in the samples. The oldest zircon dates at 2470 ± 10 Ma; no Archean dates were found. Four zircons date between 2103 ± 5 Ma and 1952 ± 11 Ma, 20 date between 1094 ± 10 Ma and 899 ± 6 Ma (36%), and 31 date between 794 ± 16 Ma and 579 ± 14 Ma (55%) representing the most abundant age-population. The probability plot shows two major peaks at 1000 Ma and 670 Ma (Fig. 5C).

Samples D470, D600 and WP19 (the Lower Kwango Group)

In samples D470, D600 and WP19, from aeolian red sandstones of the Lower Kwango Group, zircons are generally medium in size, well sorted, well rounded and often transparent (Fig. 4D). Few are small, yellowish and with crystal shapes.

148 analyses were performed on 137 grains in samples D470 and D600 from the upper part of the Dekese section (Tables 6 and 7). In total 94 single zircon dates are concordant in these two samples. The seven oldest zircons date between 2630 ± 16 Ma and 2473 ± 16 Ma, one dates at 2.1 Ga (2154 ± 16 Ma), and eight date between 2080 ± 17 Ma and 1788 ± 22 Ma (8%). One zircon dates at 1.5 Ga (1548 ± 13 Ma), 27 date between 1272 ± 23 Ma and 884 ± 19 Ma (29%), and 49 date between 837 ± 21 Ma and 513 ± 21 Ma (52%) that represent the most abundant age-population (Fig. 5D). Following this distribution, the probability plot shows four peaks at 2580 Ma, 2000 Ma, 970 Ma and 680 Ma. The two youngest zircons have $^{206}\text{Pb}/^{238}\text{U}$ dates of 286 ± 7 Ma and 240 ± 6 Ma, concordant at 89% and 99%, respectively (Table 6).

In sample WP19, from Kwango red sandstones outcropping at a cliff near Swamasangu (Fig. 3A), 66 analyses were performed on 64 grains (Table 8). 54 single zircon dates are concordant. The oldest zircon dates at 3133 ± 29 Ma, four date at 2.6 Ga, and nine date between 2212 ± 28 Ma and 1766 ± 30 Ma (16%). 16 zircons are bracketed between 1044 ± 33 Ma and 922 ± 34 Ma (28%), and 22 date between 851 ± 34 Ma and 544 ± 37 Ma (41%) representing the most abundant age-population (Fig. 5E). One young zircon dates at 426 ± 8 Ma ($^{206}\text{Pb}/^{238}\text{U}$ date concordant at 106%), and two younger $^{206}\text{Pb}/^{238}\text{U}$ date at 200 ± 10 Ma and 190 ± 10 Ma, concordant at 79% and 95%, respectively (Table 8).

Sample WP103 (the Kalahari Group)

Sample WP103 is taken from locally mined (diamondiferous) gravels of the Kalahari Group at Kitsaku Digging in the Kwango area (Fig. 3B). In this sample, zircons are coarse to very coarse (300-600 μm), both angular and well rounded, and of various color (Fig. 4E). In total 50 single zircon dates are concordant (Table 9). 31 date between 2958 ± 26 Ma and 2491 ± 27 Ma (62%), which represent the most abundant age-population (Fig. 5F). Three zircons date between 2294 ± 29 Ma and 2158 ± 28 Ma, five date at 1.9 Ga, one dates at 1.0 Ga (1058 ± 20 Ma), and nine are between 734 ± 34 Ma and 529 ± 36 Ma (18%). Two young zircons have $^{206}\text{Pb}/^{238}\text{U}$ dates of 300 ± 10 Ma ($^{206}\text{Pb}/^{238}\text{U}$ dates concordant at 79% and 91%), and the two youngest, which are large

1 zircon fragments with very low U and Pb concentrations, date at 130-140 Ma
2 (concordant at 12% and 34%). The latter could represent fragments of kimberlitic
3 megacrysts but more analysis is needed to support this interpretation.
4
5
6

7 **5. Discussion**

8
9 In the different stratigraphic groups of the CB (the Inkisi, Lukuga, Haute Lueki,
10 Kwango and Kalahari Groups) four main detrital zircon age-populations are found
11 (Fig. 6A): 1) Archean to early Paleoproterozoic; 2) mid-Paleoproterozoic (Eburnian);
12 3) mid-Mesoproterozoic to early Neoproterozoic (Kibaran); and 4) late
13 Neoproterozoic to early Cambrian (Pan African), although there are differences in
14 their proportions. The occurrence of a small number (6) of Carboniferous-Jurassic
15 zircons within the uppermost Kwango and Kalahari Groups suggests the emergence
16 of younger source terrains during the late Mesozoic. This change coincides with the
17 conspicuous (break-up) unconformity at the base of the Jurassic-Cretaceous
18 succession in the CB (Fig. 2).
19
20
21
22
23
24
25
26

27 [Figure 6 here]
28
29

30 **Archean to early Paleoproterozoic (3.1 Ga and 2.9-2.4 Ga)**

31 Archean to early Paleoproterozoic dates are present in all the samples, albeit not the
32 most abundant (13% in total; Fig. 6A). The oldest zircon dates at 3.1 Ga (3133 ± 29
33 Ma), and the others range between 2959 ± 26 Ma and 2428 ± 16 Ma. These dates are
34 the most abundant in the samples from the Kwango field study area and from the
35 Dekese section (only one grain is from the Samba section). They may have been
36 derived from a number of cratonic sources surrounding the CB (Fig. 6B; see de Wit
37 and Linol, 2014, for review), for example: the ca. 2.9-2.7 Ga Kasai-Lomami and
38 Dibaya Complexes of the Kasai and Cuango Cratons (Cahen et al, 1984; Delhal,
39 1991); the 3.2-2.7 Ga Ntem Complex and Nyong Series (Caen-Vachette et al., 1988;
40 Feybesse et al., 1998; Nkoumbou et al., 2013), the 3.0-2.6 Ga Mboumou-Uganda
41 Craton (Link et al., 2010; Mänttari et al., 2013), the Tanzanian Craton (e.g. the 3.1-2.5
42 Ga Dodoman Complex; Kabete et al. 2012; Lawley et al., 2013). Other possible
43 sources are from surrounding Proterozoic belts, such as for example from the Mbuji-
44 Mayi and Muva sequences in southeastern DRC, which contain Archean detrital
45 zircons (Rainaud et al., 2003; Delpomdor et al., 2013). In the sample from the
46 (Kalahari) Kwango river terraces, however, the predominant dates of 2715 Ma most
47
48
49
50
51
52
53
54
55
56
57
58
59
60
61
62
63
64
65

1 likely correspond to migmatites and pegmatites of the Dibaya Complex (the Cuango
2 Craton), outcropping immediately upstream along a major knickpoint, as indicated by
3 the large size and angular shape of the zircons (Fig. 5F).
4
5

6 **Mid-Paleoproterozoic (2.2-1.8 Ga)**

7
8 Mid-Paleoproterozoic dates are represented in all the samples (18% in total; Fig. 6A),
9 but are much more abundant in the samples from the Lukuga diamictites in the
10 Dekese section (Fig. 5B). These dates, mainly ranging between 2.0 Ga and 1.8 Ga,
11 correspond to widely outcropping Eburnian rock sequences in east Africa (e.g. the
12 Toro and Ubendian Belts; Link et al., 2010; Boniface et al., 2012), as indicated by the
13 westward direction of paleocurrents for the Lukuga Group (Fig. 6B).
14
15
16
17
18
19

20 **Mesoproterozoic to early Neoproterozoic to (1600-850 Ma)**

21 Mesoproterozoic to early Neoproterozoic dates are abundant in all the samples (33%
22 in total; Fig. 6A), indicating important and prolonged contributions from Kibaran
23 aged-terrains to the sediment sources for the CB. In the samples from the Lukuga
24 Group five zircons dated between 1421 ± 16 Ma and 1371 ± 18 Ma. This coincides
25 with the Kibaran-age Belt (*sensu stricto*) along the eastern margin of the basin (Fig.
26 6B), dated at ca. 1375 Ma (Tack et al., 2010). The lack of detrital zircons of this age
27 (1.4 Ga) in all the other samples suggests that this large region of east-central Africa
28 was not a major source for the CB, possibly because it was covered by later sediments
29 or because it remained below sea level.
30
31
32
33
34
35
36
37

38 In all samples from all the stratigraphic sequences, most of other dates are bracketed
39 between 1100 Ma and 950 Ma (Fig. 6A). In addition, repeated analysis on some
40 zircons of this age also gave younger dates of 750 Ma, 700 Ma and 650 Ma, providing
41 evidence for local recrystallization during the late Neoproterozoic. This suggests
42 partial reworking during the Pan African orogens. Such dates are most common
43 within the Oubanguides, in particular the ca. 1000-600 Ma Central Saharan Belt in
44 CAR and North African Shield (e.g. in Chad; de Wit et al., 2005, and 2014; Toteu et
45 al., in preparation), and on the South American flank of the Atlantic Ocean, especially
46 within the Sergipano-Araguaia Belts in northeastern Brazil (e.g. dos Santos et al.,
47 2010; de Brito Neves, 2011). These (distant) northern provenances for the CB are
48 supported by other recent detrital zircon studies that found also dominant 1.0 Ga age-
49 populations within the upper Neoproterozoic to lower Paleozoic West Congo and
50 Inkisi Groups along the western margin of the basin (Frimmel et al., 2006; Jelsma et
51
52
53
54
55
56
57
58
59
60
61
62
63
64
65

1
2
3
4
5
6
7
8
9
10
11
12
13
14
15
16
17
18
19
20
21
22
23
24
25
26
27
28
29
30
31
32
33
34
35
36
37
38
39
40
41
42
43
44
45
46
47
48
49
50
51
52
53
54
55
56
57
58
59
60
61
62
63
64
65

al., 2011). Such Pan African metasediments and associated molasses-like basin sequences, abundantly exposed around the margins of the CB, and which were regionally derived from the north (Alvarez et al., 1995; Master et al., 2005; Figs. 6B and 7), may also have constituted significant secondary sources for the sediments.

Late Neoproterozoic to Cambrian (850-500 Ma)

Late Neoproterozoic to Cambrian zircon dates are also abundant in all the samples (35% in total; Fig. 6A). This series of dates, relatively continuous between 800 Ma and 540 Ma, corresponds to several episodes of the Pan African orogens. However, possible sources with this age-range are abundant within the Pan African mobile belts that surround the CB, and at this stage it is not possible to differentiate between these widely dispersed terrains. Sediment dispersal directions (Fig. 6B) favor Pan African provinces located to the north (the Oubanguides), and to the east and southeast (the Mozambique and Lufilian Belts). In addition, the general increase in abundance of this 850-500 Ma zircon age-population from the Paleozoic (Inkisi and Lukuga) to the Mesozoic sequences (Haute Lueki and Kwango) could suggest sustained Phanerozoic exhumation of the surrounding Pan African mobile belts, and/or progressive concentration by recycling Paleozoic sediments (Fig. 7).

[Figure 7 here]

Late Carboniferous-Jurassic (300-240 and 190 Ma)

Six young zircons, small in size and displaying no magmatic zoning, dated at 300-240 Ma and 190 Ma in the Kwango and Kalahari Groups indicate some contributions from Upper Carboniferous-Lower Jurassic sources to the CB. These dates may possibly correspond to Permian-Triassic kimberlites and Karoo flood basalts in northern Angola (Jelsma personal communication in 2011). However, it is more likely that these fine and delicate zircons are related to ash fallouts linked to extensive late Paleozoic-Jurassic felsic volcanism and magmatism of the Choiyoi and Chon Aike Provinces in western Argentina and Chile (Mpodozis and Kay, 1992; Ramos and Aleman, 2000; Munizaga et al., 2008). For instance, such air-fall tuffs are commonly recorded in the Permian-Triassic sedimentary rocks of the Paraná and Karoo Basins of southwestern Gondwana (Bangert et al., 1999; Guerra-Sommer et al., 2008; Milani and de Wit, 2008; Fildani et al., 2009; Rocha-Campos et al., 2011). In the southern CB, however, paleo-wind directions measured from the Kwango aeolianites (e.g. Fig. 3A) indicate strong near surface winds to the southwest. Thus, this suggests

1 (opposite) north-directed upper atmospheric circulations across interior Gondwana,
2 episodically transporting volcanic dust originated from volcanoes above the Andean
3 subduction margin of Gondwana, more than 5000 km northward to the CB (Fig. 8).
4

5 [Figure 8 here]
6
7
8
9

10 **Conclusions**

11 U-Pb dates from 568 detrital zircons of the Phanerozoic successions in the CB
12 characterize the evolution of source provenances during the development of this
13 largest basin of central Gondwana. The four main age-populations documented in this
14 study (ca. Archean, Eburnian, Kibaran and Pan African) can be linked to potential
15 sources within the Precambrian basement immediately surrounding the CB. An
16 exception is a prominent peak at 950-1100 Ma (Fig. 6A), for which the most likely
17 (larger) sources are within the Oubanguides and the North African Shield (e.g.
18 Darfour), and the Brasiliano Belts in northeastern Brazil, since their upper
19 Neoproterozoic sequences and associated sedimentary cover are widespread around
20 the CB and given that these sequences regionally derived from the north. In contrast,
21 input from the ca. 1.4 Ga Kibaran Belt is limited to the east-derived, Carboniferous
22 glacial deposits of the CB. This suggests that east-central Africa was mostly not a
23 major source for the sediments, possibly because this region was covered by
24 sediments or remained below sea-level throughout the late Paleozoic-Mesozoic, as
25 supported by sedimentological and biostratigraphic data. In addition, some younger
26 zircons dated at 290 Ma, 240 Ma, 200 Ma and 190 Ma in the Jurassic-Cretaceous
27 aeolian red sandstones reflects the influence of new Permian-Jurassic sources during
28 the Mesozoic. We interpret those to be derived from air-fall tuffs related to far-field
29 volcanic activity of the proto-Andes flanking the southwest margin of Gondwana
30 (Figs. 7 and 8).
31
32
33
34
35
36
37
38
39
40
41
42
43
44
45
46
47
48
49

50 **Acknowledgments**

51 We acknowledge funding through the Inkaba yeAfrica and !Khure Africa programs,
52 supported by the DST/NRF of South Africa. We thank Max Fernandez-Alonso,
53 Damien Delvaux and Edmond Thorose for accessing the archived cores at the Royal
54 Museum for Central Africa (RMCA), and Ulrich Glasmacher for providing some of
55 the zircon concentrates from the lower parts of the boreholes. B. Linol particularly
56
57
58
59
60
61
62
63
64
65

thanks Hielke Jelsma for discussions about the CB. We also thank S. Master and an anonymous reviewer for their comments. This is AEON contribution number 136 and Inkaba yeAfrica contribution number 115.

1
2
3
4
5
6
7
8
9
10
11
12
13
14
15
16
17
18
19
20
21
22
23
24
25
26
27
28
29
30
31
32
33
34
35
36
37
38
39
40
41
42
43
44
45
46
47
48
49
50
51
52
53
54
55
56
57
58
59
60
61
62
63
64
65

References

1
2 Alvarez, P., Maurin, J.C., and Vicat, J.-P., 1995. La Formation de l'Inkisi
3 (Supergroupe Ouest-congolien) en Afrique centrale (Congo et Bas-Zaïre): un delta
4 d'âge Paléozoïque comblant un bassin en extension. *Journal of African Earth*
5 *Sciences*, 20(2), p.119-131.

6
7
8
9 Antunes, M.T., Maisey, J.G., Marques, M.M., Schaeffer, B., and Thomson, K.S.,
10 1990. Triassic fishes from the Cassange Depression (R.P. de Angola). *Universidade de*
11 *Lisboa, Ciencias da Terra, Numero Esp*, p.1-64.

12
13
14
15 Bangert, B., Stollhofen, H., Lorenz, V., and Armstrong, R., 1999. The
16 geochronology and significance of ash-fall tuffs in the glaciogenic Carboniferous-
17 Permian Dwyka Group of Namibia and South Africa. *Journal of African Earth*
18 *Sciences*, 29(1), p.33-49.

19
20
21
22 Belshaw, N.S., Freedman, P.A., O'Nions, R.K., Frank, M., and Guo, Y., 1998. A
23 new variable dispersion double-focussing plasma mass spectrometer with
24 performance illustrated for Pb isotopes. *International Journal of Mass Spectrometry*,
25 181, p.51-58.

26
27
28
29 Biggin, A.J., de Wit, M.J., Langereis, C.G., Zegers, T.E., Voûte, S., Dekkers, M.J.,
30 and Drost, K., 2011. Palaeomagnetism of Archean rocks of the Onverwacht Group,
31 Barberton Greenstone Belt (southern Africa): Evidence for a stable and potentially
32 reversing geomagnetic field at ca. 3.5 Ga. *Earth and Planetary Science Letters*, 302(3-
33 4), p.314-328.

34
35
36
37 Bingen, B., Jacobs, J., Viola, G., Henderson, I.H.C., Skår, Ø., Boyd, R., Thomas,
38 R.J., Solli, A., Key, R.M., and Daudi, E.X.F., 2009. Geochronology of the
39 Precambrian crust in the Mozambique belt in NE Mozambique, and implications for
40 Gondwana assembly. *Precambrian Research*, 170(3-4), p.231-255.

41
42
43
44 Boniface, N., Schenk, V., Appel, P. 2012. Paleoproterozoic eclogites of MORB-
45 type chemistry and three Proterozoic orogenic cycles in the Ubendian Belt
46 (Tanzania): Evidence from monazite and zircon geochronology, and geochemistry.
47 *Precambrian Research* 192-195, p.16– 33.

48
49
50
51
52
53
54
55
56
57
58
59
60
61
62
63
64
65
66
67
68
69
70
71
72
73
74
75
76
77
78
79
80
81
82
83
84
85
86
87
88
89
90
91
92
93
94
95
96
97
98
99
100
101
102
103
104
105
106
107
108
109
110
111
112
113
114
115
116
117
118
119
120
121
122
123
124
125
126
127
128
129
130
131
132
133
134
135
136
137
138
139
140
141
142
143
144
145
146
147
148
149
150
151
152
153
154
155
156
157
158
159
160
161
162
163
164
165
166
167
168
169
170
171
172
173
174
175
176
177
178
179
180
181
182
183
184
185
186
187
188
189
190
191
192
193
194
195
196
197
198
199
200
201
202
203
204
205
206
207
208
209
210
211
212
213
214
215
216
217
218
219
220
221
222
223
224
225
226
227
228
229
230
231
232
233
234
235
236
237
238
239
240
241
242
243
244
245
246
247
248
249
250
251
252
253
254
255
256
257
258
259
260
261
262
263
264
265
266
267
268
269
270
271
272
273
274
275
276
277
278
279
280
281
282
283
284
285
286
287
288
289
290
291
292
293
294
295
296
297
298
299
300
301
302
303
304
305
306
307
308
309
310
311
312
313
314
315
316
317
318
319
320
321
322
323
324
325
326
327
328
329
330
331
332
333
334
335
336
337
338
339
340
341
342
343
344
345
346
347
348
349
350
351
352
353
354
355
356
357
358
359
360
361
362
363
364
365
366
367
368
369
370
371
372
373
374
375
376
377
378
379
380
381
382
383
384
385
386
387
388
389
390
391
392
393
394
395
396
397
398
399
400
401
402
403
404
405
406
407
408
409
410
411
412
413
414
415
416
417
418
419
420
421
422
423
424
425
426
427
428
429
430
431
432
433
434
435
436
437
438
439
440
441
442
443
444
445
446
447
448
449
450
451
452
453
454
455
456
457
458
459
460
461
462
463
464
465
466
467
468
469
470
471
472
473
474
475
476
477
478
479
480
481
482
483
484
485
486
487
488
489
490
491
492
493
494
495
496
497
498
499
500
501
502
503
504
505
506
507
508
509
510
511
512
513
514
515
516
517
518
519
520
521
522
523
524
525
526
527
528
529
530
531
532
533
534
535
536
537
538
539
540
541
542
543
544
545
546
547
548
549
550
551
552
553
554
555
556
557
558
559
560
561
562
563
564
565
566
567
568
569
570
571
572
573
574
575
576
577
578
579
580
581
582
583
584
585
586
587
588
589
590
591
592
593
594
595
596
597
598
599
600
601
602
603
604
605
606
607
608
609
610
611
612
613
614
615
616
617
618
619
620
621
622
623
624
625
626
627
628
629
630
631
632
633
634
635
636
637
638
639
640
641
642
643
644
645
646
647
648
649
650
651
652
653
654
655
656
657
658
659
660
661
662
663
664
665
666
667
668
669
670
671
672
673
674
675
676
677
678
679
680
681
682
683
684
685
686
687
688
689
690
691
692
693
694
695
696
697
698
699
700
701
702
703
704
705
706
707
708
709
710
711
712
713
714
715
716
717
718
719
720
721
722
723
724
725
726
727
728
729
730
731
732
733
734
735
736
737
738
739
740
741
742
743
744
745
746
747
748
749
750
751
752
753
754
755
756
757
758
759
760
761
762
763
764
765
766
767
768
769
770
771
772
773
774
775
776
777
778
779
780
781
782
783
784
785
786
787
788
789
790
791
792
793
794
795
796
797
798
799
800
801
802
803
804
805
806
807
808
809
810
811
812
813
814
815
816
817
818
819
820
821
822
823
824
825
826
827
828
829
830
831
832
833
834
835
836
837
838
839
840
841
842
843
844
845
846
847
848
849
850
851
852
853
854
855
856
857
858
859
860
861
862
863
864
865
866
867
868
869
870
871
872
873
874
875
876
877
878
879
880
881
882
883
884
885
886
887
888
889
890
891
892
893
894
895
896
897
898
899
900
901
902
903
904
905
906
907
908
909
910
911
912
913
914
915
916
917
918
919
920
921
922
923
924
925
926
927
928
929
930
931
932
933
934
935
936
937
938
939
940
941
942
943
944
945
946
947
948
949
950
951
952
953
954
955
956
957
958
959
960
961
962
963
964
965
966
967
968
969
970
971
972
973
974
975
976
977
978
979
980
981
982
983
984
985
986
987
988
989
990
991
992
993
994
995
996
997
998
999
1000

1 Bose, M.N., and Kar, R.K., 1976. Palaeozoic *spora dispersa* from Zaïre
2 (Congo). XI: Assises glaciaires et periglaciaire from the Lukuga Valley. Annales du
3 Musée Royal de l'Afrique centrale, Tervuren (Belgique), Série in 8, Sciences
4 Géologiques, 77, p.1-19.

5
6
7 Bose, M.N., and Kar, R.K., 1978. Biostratigraphy of the Lukuga Group in Zaïre.
8 Annales du Musée Royal de l'Afrique centrale, Tervuren (Belgique), Série in 8,
9 Sciences Géologiques, 82, p.97-114.

10
11
12 Boulouard, C., and Calandra, F., 1963. Etude palynologique de quelques sondages
13 de la République du Congo (Congo ex-Belge). Unpublished report R/ST-no.7376,
14 SNPA Direction exploration et production Pau, France.

15
16
17
18 Boutakoff, N., 1948. Les formations glaciaires et post-glaciaires fossilifères, d'âge
19 permo-carbonifère (Karoo inférieur) de la région de Walikale (Kivu, Congo belge).
20 Mémoire de l'Institut géologique. Université de Louvain, IX (II), 214 pp.

21
22
23
24
25
26
27
28
29
30
31
32
33
34
35
36
37
38
39
40
41
42
43
44
45
46
47
48
49
50
51
52
53
54
55
56
57
58
59
60
61
62
63
64
65

Buiter, S.J.H., Steinberger, B., Medvedev, S., and Tetreault, J.L., 2012. Could the
mantle have caused subsidence of the Congo Basin? Tectonophysics, 514-517, p.62-
80.

Caen-Vachette, M., Vialette, Y., Bassot, J.-P., and Vidal, P., 1988. Apport de la
géochronologie isotopique à la connaissance de la géologie gabonaise. Chroniques de
la recherche minière, 491, p.35-54.

Cahen, L., 1954. Géologie du Congo Belge. Liège: Vaillant-Carmanne, 577pp.

Cahen, L., 1981. Précisions sur la stratigraphie et les corrélations du Groupe de la
Haute-Lueki et des formations comparables (Triasique à Liasique? d'Afrique
Centrale). Rapport annuel du Musée Royal d'Afrique centrale, Tervuren (Belgique),
Département de Géologie et de Minéralogie, p.81-96.

Cahen, L., 1983a. Le Groupe de Stanleyville (Jurassique supérieur et Wealdien de
l'intérieur de la République du Zaïre): Révision des connaissances. Rapport annuel du
Musée Royal de l'Afrique centrale, Tervuren (Belgique), Département de Géologie et
de Minéralogie, p.73-91.

Cahen, L., 1983b. Brèves précisions sur l'âge des groupes crétaciques post-
Wealdien (Loia, Bokungu, Kwango) du Bassin intérieur du Congo (République du
Zaïre). Rapport annuel du Musée Royal de l'Afrique centrale, Tervuren (Belgique),
Département de Géologie et de Minéralogie, p.61-72.

Cahen, L., and Lepersonne, J., 1978. Synthèse des connaissances relatives au
Groupe (anciennement Série) de la Lukuga (Permien du Zaïre). Annales du Musée

1
2
3
4
5
6
7
8
9
10
11
12
13
14
15
16
17
18
19
20
21
22
23
24
25
26
27
28
29
30
31
32
33
34
35
36
37
38
39
40
41
42
43
44
45
46
47
48
49
50
51
52
53
54
55
56
57
58
59
60
61
62
63
64
65

Royal du Congo belge, Tervuren (Belgique), Série in-8, Sciences géologiques, 82, p.115-152.

Cahen, L., Ferrand, J.J., Haarsma, M.J.F., Lepersonne, J., and Verbeek, T., 1959. Description du Sondage de Samba. Annales du Musée Royal du Congo belge, Tervuren (Belgique), Série in-8, Sciences géologiques, 29, 210p.

Cahen, L., Ferrand, J.J., Haarsma, M.J.F., Lepersonne, J., and Verbeek, T., 1960. Description du Sondage de Dekese. Annales du Musée Royal du Congo belge, Tervuren (Belgique), Série in-8, Sciences géologiques, 34, 115p.

Cahen, L., Snelling, N.J., Delhal, J., and Vail, J., 1984. The Geochronology and Evolution of Africa. Oxford: Clarendon Press, 512pp.

Casier, E., 1965, Poissons fossiles de la Série du Kwango (Congo). Annales du Musée royal de l'Afrique Centrale, Tervuren (Belgique), Série in-8, Sciences géologiques, 50, 69p.

Catuneanu, O., Wopfner, H., Eriksson, P.G., Cairncross, B., Rubidge, B.S., Smith, R.M.H., and Hancox, P.J., 2005. The Karoo basins of south-central Africa. Journal of African Earth Sciences, 43(1-3), p.211-253.

Cocherie, A., and Robert, M., 2008. Laser ablation coupled with ICP-MS applied to U-Pb zircon geochronology: A review of recent advances. Gondwana Research, 14, p.597-608.

Colin, J.-P., 1981. Paleontological study of the Esso/Texaco well Gilson-1, Zaire. Unpublished report EPR-E.WA19.81.

Colin, J.-P., 1994. Mesozoic-Cenozoic lacustrine sediments in the Zaire Interior Basin. In: Gierlowski-Kordesch, E., and Kelts, K. (eds.), Global Geological Record of Lake Basins. Cambridge University Press, 4, pp.31-36.

Colin, J.-P., and Jan du Chêne, J., 1981. Paleontological study of the Esso/Texaco well Mbandaka-1, Zaire. Unpublished report EPR-E.WA15.81.

Cox, L.R., 1960. Further mollusca from the Lualaba beds of the Belgian Congo. Annales du Musée Royal du Congo belge, Tervuren (Belgique), 37, p.1-15.

Crosby, A. G., Fishwick, S., and White, N., 2010. Structure and evolution of the intracratonic Congo Basin. Geochemistry Geophysics Geosystems, 11(6), p.1-20.

Daly, M.C., Lawrence, S.R., Kimun'a, D., and Binga, M., 1991. Late Paleozoic deformation in central Africa: a result of distant collision. Nature, 350, p.605-607.

1
2
3
4
5
6
7
8
9
10
11
12
13
14
15
16
17
18
19
20
21
22
23
24
25
26
27
28
29
30
31
32
33
34
35
36
37
38
39
40
41
42
43
44
45
46
47
48
49
50
51
52
53
54
55
56
57
58
59
60
61
62
63
64
65

Daly, M.C., Lawrence, S.R., Diemu-Tshiband, K., and Matouana, B., 1992. Tectonic evolution of the Cuvette Centrale, Zaire. *Journal of the Geological Society*, 149(4), p.539-546.

De Brito Neves, B.B., 2011. The Paleoproterozoic in the South-American continent: Diversity in the geologic time. *Journal of South American Earth Sciences*, 32, p.270-286.

De Carvalho, H., Tassinari, C., Alves, P.M., Guimarães, F., and Simões, M.C., 2000. Geochronological review of the Precambrian in western Angola: links with Brazil. *Journal of African Earth Sciences*, 31(2), p.383-402.

Defretin-Lefranc, S., 1967. Étude sur les phyllopoïdes du Bassin du Congo. *Annales du Musée Royal de l'Afrique centrale, Tervuren (Belgique), Série in-8, Sciences géologiques*, 56, 122p.

Delhal, J., 1991, Situation géochronologique 1990 du Précambrien du Sud-Kasai et de l'Ouest-Shaba. Rapport annuel du Musée Royal de l'Afrique centrale, Tervuren (Belgique), Département de Géologie et de Minéralogie, p.119-125.

Delpomdor, F., Linnemann, U., Boven, A., Gärtner, A., Travin, A., Blanpied, C., Virgone, A., Jelsma, H., and Prémat, A., 2013. Depositional age, provenance, and tectonic and paleoclimatic settings of the late Mesoproterozoic-middle Neoproterozoic Mbuji-Mayi Supergroup, Democratic Republic of Congo. *Palaeogeography, Palaeoclimatology, Palaeoecology*, 389, p.4-34.

De Ploey, J., 1968. Sédimentologie et origine des sables de la série des sables ocre et de la série des 'grès polymorphes' (Système du Kalahari) au Congo Occidental. *Annales du Musée Royal de l'Afrique centrale, Tervuren (Belgique), Série in-8, Sciences géologiques*, 61, 72p.

De Waele, B., Johnson, S.P., and Pisarevsky, S.A., 2008. Palaeoproterozoic to Neoproterozoic growth and evolution of the eastern Congo Craton: Its role in the Rodinia puzzle. *Precambrian Research*, 160, p.127-141.

De Waele, B., Liégeois, J.-P., Nemchin, A.A., and Tembo, F., 2006. Isotopic and geochemical evidence of Proterozoic episodic crustal reworking within the Irumide belt of south-central Africa, the southern metacratonic boundary of an Archaean Bangweulu Craton. *Precambrian Research*, 148(3-4), p.225-256.

De Wit, M.J., 2009. Tsodilo Resources Limited drills extension of Zambian copper belt-like mineralization in Pan African Basement of northwest Botswana. Tsodilo Resources Ltd. Report. www.tsodiloresources.com

1 De Wit, M.J., Jeffery, M., Berg, H, and Nicolayson, L.O., 1988. Geological Map
2 of sectors of Gondwana re-constructed to their position ~150 Ma (with explanatory
3 notes), scale 1: 1.000.000. Tulsa: American Association of Petroleum Geologists.
4

5 De Wit, MJ, Bowring, S., Dudas, F., Kamga, G. 2005. The great Neoproterozoic
6 central Saharan arc and the amalgamation of the north African Shield. GAC-MAC-
7 CSPG-CSSS Conference, Halifax, Canada. Abstracts with programs, p43.
8
9

10 De Wit, M.J., de Brito Neves, B.B., Trouw, R.A.J., and Pankhurst, R.J., 2008. Pre-
11 Cenozoic correlations across the South Atlantic region: “the ties that bind”. In:
12 Pankurst, R.J., Trouw, R.A.J., Brito Neves, B.B., and de Wit, M.J. (eds.), West
13 Gondwana: Pre-Cenozoic Correlations Across the South Atlantic Region. Geological
14 Society of London, Special Publications, 294, pp.1-8.
15
16
17
18
19

20 De Wit, M.J., and Linol, B., 2014. Chapter 2: Precambrian basement of the Congo
21 Basin and its flanking terrains. In: de Wit, M.J., Guillocheau, F., and de Wit, M.J.C.
22 (Eds.), The Geology and Resource Potential of the Congo Basin, Springer-Verlag, in
23 press.
24
25
26

27 De Wit, M.J., Bowring, S., Buchwaldt, R., Dudas, F., MacPhee, D, Tagne-Kamga,
28 G., Dunn, N., Salet, A.M., and Nambatingar, D. 2014. Proterozoic crust of the Central
29 Sahara Shield. (Submitted to Gondwana Research).
30
31

32 Dos Santos, E.J., von Schmus, W.R.V., Kozuch, M., and Neves, B.B.D.B., 2010.
33 The Cariris Velhos tectonic event in Northeast Brazil. Journal of South American
34 Earth Sciences, 29(1), p.61-76.
35
36
37

38 Esso-Zaire SARL, 1981a. Geological Completion Report: Gilson-1. Unpublished
39 report.
40

41 Esso-Zaire SARL, 1981b. Geological Completion Report: Mbandaka-1.
42 Unpublished report.
43
44

45 Evrard, P., 1960. Sismique. Annales du Musée Royal du Congo belge, Tervuren
46 (Belgique), Série in-8, Sci-ences géologiques, 33, 87p.
47
48

49 Fedo, C.M., Sircombe, K.N., and Rainbird, R.H., 2003. Detrital zircon analysis of
50 the sedimentary record. Reviews in Mineralogy and Geochemistry, 53(1), p.277-303.
51

52 Fernandez-Alonso, A., Cutten, H., De Waele B., Tack, L., Tahon, A., Baudet, D.,
53 and Barritt, S.D., 2012. The Mesoproterozoic Karagwe-Ankole Belt (formerly the NE
54 Kibara Belt): The result of prolonged extensional intracratonic basin development
55 punctuated by two short-lived far-field compressional events. Precambrian Research,
56 216-219, p.63-86.
57
58
59
60
61
62
63
64
65

1 Feybesse, J.L., Johan, V., Triboulet, C., Guerrot, C. Mayaga-Mikolo, F., Bouchot,
2 V., Eko N'Dong, J., 1998. The West Central African belt: a model of 2.5-2.0 Ga
3 accretion and two-phase orogenic evolution. *Precambrian Research*, 87, p.161-216.
4

5 Fildani, A., Weislogel, A., Drinkwater, N.J., McHargue, T., Tankard, A., Wooden,
6 J., Hodgson, D., and Flint, S., 2009. U-Pb zircon ages from the southwestern Karoo
7 Basin, South Africa: Implications for the Permian-Triassic boundary. *Geology*, 37(8),
8 p.719-722.
9

10 Frimmel, H., Tack, L., Basei, M., Nutman, A, and Boven, A, 2006. Provenance
11 and chemostratigraphy of the Neoproterozoic West Congolian Group in the
12 Democratic Republic of Congo. *Journal of African Earth Sciences*, 46(3), p.221-239.
13

14 Fritz, H., Abdelsalam, M., Ali, K.A., Bingen, B., Collins, A.S., Fowler, A.R.,
15 Ghebreab, W., Hauenberger, C.A., Johnson, P.R., Kusky, T.M., P. Macey, P., S.
16 Muhongo, S., Stern, R.J., Viola, G. 2013. Orogen styles in the East African Orogen:
17 A review of the Neoproterozoic to Cambrian tectonic evolution. *Journal of African*
18 *Earth Sciences*, 86, 65–106.
19

20 Giresse, P., 2005. Mesozoic-Cenozoic history of the Congo Basin. *Journal of*
21 *African Earth Sciences*, 43, p.301-315.
22

23 Grékoff, N., 1957. Ostracodes du Bassin du Congo. I. Jurassique supérieur et
24 Crétacé inférieur du nord du bassin. *Annales du Musée Royal de l’Afrique centrale*,
25 Tervuren (Belgique), Série in-8, Sciences géologiques, 19, 97p.
26

27 Grékoff, N., 1958. Ostracodes du Bassin du Congo. III. Tertiaire. *Annales du*
28 *Musée Royal de l’Afrique centrale*, Tervuren (Belgique), Série in-8, Sciences
29 géologiques, 22, 36p.
30

31 Grékoff, N., 1960. Ostracodes du Bassin du Congo. II. Crétacé. *Annales du Musée*
32 *Royal de l’Afrique centrale*, Tervuren (Belgique), Série in-8, Sciences géologiques,
33 22, 36p.
34

35 Guerra-Sommer, M., Cazzulo-Klepzig, M., Laquintinie Formoso, M.L., Menegat,
36 R., and Mendonça Fo, J.G., 2008. U-Pb dating of tonstein layers from a coal
37 succession of the southern Paraná Basin (Brazil): A new geochronological approach.
38 *Gondwana Research*, 14(3), p.474-482.
39

40 Jamal, D.L., 2005. Crustal studies across selected geotransects in NE
41 Mozambique: Differentiating between Mozambican (-Kibaran) and Pan Africa
42 events, with implications for Gondwana studies. Unpublished PhD Thesis, University
43 of Cape Town, 365 pp.
44
45
46
47
48
49
50
51
52
53
54
55
56
57
58
59
60
61
62
63
64
65

1 Jamotte, A., 1932. Contribution à l'étude géologique du bassin charbonnier de la
2 Lukuga. Annales du Service des Mines, Tome II, Comité Spécial du Katanga, p.1-75.

3 Jelsma, H.A, Perrit, S.H., Armstrong, R., and Ferreira, H.F., 2011. Shrimp U-Pb
4 zircon geochronology of basement rocks of the Angolan Shield, western Angola.
5 Abstract, 23rd CAG, Johannesburg, 8th-14th January.
6

7 Johnson, M.R., van Vuuren, C.J., Hegenberger, W.F., Key, R., and Shoko, U.,
8 1996. The Stratigraphy of the Karoo Supergroup in southern Africa: an overview.
9 Journal of African Earth Sciences, 23(1), p.3-15.
10

11 Jokat, W., Boebel, T., König, M., and Meyer, U., 2003. Timing and geometry of
12 early Gondwana breakup. Journal of Geophysical Research: Solid Earth, 108(B9).
13

14 Jones, L., Mathieu, P.L., and Strenger, H., 1959. Magnétisme. Annales du Musée
15 Royal de l'Afrique central, Tervuren (Belgique), Série in-8, Sciences géologiques, 27,
16 30p.
17

18 Kadima, E., Delvaux, D., Sebagenzi, S.N., Tack, L., and Kabeya, S.M., 2011.
19 Structure and geological history of the Congo Basin: an integrated interpretation of
20 gravity, magnetic and reflection seismic data. Basin Research, 23(5), p.499-527.
21

22 Kamo, S.L., and Davis, D.W., 1994. Reassessment of Archean crustal
23 development in the Barberton Mountain Land, South Africa, based on U-Pb dating.
24 Tectonics, 13(1). P.167-192.
25

26 Kanda N.V., Mpiana, C., Cibambula, E., Fernandez-Alonso, M., Delvaux, D.,
27 Kadima, E., Delpomdor, F., Tahon, A., Dumont, P., Hanon, M., Baudet, D., de
28 Waele, S., and Tack, L., 2011. The 1000 m thick Redbeds sequence of the Congo
29 River Basin (CRB): a generally overlooked testimony in Central Africa of post-
30 Gondwana amalgamation (550 Ma) and pre-Karoo break-up (320 Ma). Abstract, 23rd
31 CAG, Johannesburg, 8th-14th January.
32

33 Lawley, C.J.M., Selby, D., Condon, D.J., Horstwood, M., Millar, I., Crowley, Q.,
34 Imber, J. 2013. Litho geochemistry, geochronology and geodynamic setting of the
35 Lupa Terrane, Tanzania: Implications for the extent of the Archean Tanzanian Craton.
36 Precambrian Research, 231, p.174-193.
37

38 Lawrence, S.R., and Makazu, M.M., 1988. Zaire's Central Basin: Prospectivity
39 outlook. Oil & Gas Journal, 86(38), p.105-108.
40

41 Lenoir, J.L., Liegeois, J.-P., Theunissen, K., and Klerkx, J., 1995. The
42 Palaeoproterozoic Ubendian shear belt in Tanzania: geochronology and structure.
43 Journal of African Earth Sciences, 19(3), p.169-184.
44
45
46
47
48
49
50
51
52
53
54
55
56
57
58
59
60
61
62
63
64
65

1
2
3
4
5
6
7
8
9
10
11
12
13
14
15
16
17
18
19
20
21
22
23
24
25
26
27
28
29
30
31
32
33
34
35
36
37
38
39
40
41
42
43
44
45
46
47
48
49
50
51
52
53
54
55
56
57
58
59
60
61
62
63
64
65

Lepersonne, J., 1951. Les subdivisions du système du Karoo au Kwango (Congo belge). *Annales de la Société Géologique de Belgique*, LXXIV, p.123-138.

Lepersonne, J., 1974. Carte géologique du Zaïre au 1: 2.000.000 + Notice explicative. Kinshasa, République du Zaïre: Direction de la Géologie/Musée Royal de l'Afrique centrale, Tervuren (Belgique).

Leriche, M., 1927. Les fossiles des grès polymorphes (couches de Lubilash) aux confins du Congo et de l'Angola. *Annales de la Société Géologique de Belgique*, 50, p.44-51.

Lerouge, C., Cocherie, A., Toteu, S.F., Penaye, J., Milési, J.-P., Tchameni, R., Nsifa, E.N., Fanning, C.M., and Deloule, E., 2006. Shrimp U-Pb zircon age evidence for Paleoproterozoic sedimentation and 2.05 Ga syntectonic plutonism in the Nyong Group, South-Western Cameroon: consequences for the Eburnean-Transamazonian belt of NE Brazil and Central Africa. *Journal of African Earth Sciences*, 44(4-5), p.413-427.

Link, K., Koehn, D., Barth, M.G., Aanyu, K., and Foley, S.F., 2010. Continuous cratonic crust between the Congo and Tanzania blocks in western Uganda. *International Journal of Earth Sciences (Geologische Rundschau)*, 99, p.1559-1573.

Linol, B., 2013. Sedimentology and sequence stratigraphy of the Congo and Kalahari Basins of south-central Africa and their evolution during the formation and break-up of West Gondwana. PhD thesis, Nelson Mandela Metropolitan University, 375p.

Linol, B., de Wit, M.J., Barton, E., Guillocheau, F., de Wit, M.J.C, and Colin. J.-P., 2014a. Chapter 7: Paleogeography and tectono-stratigraphy of Carboniferous-Permian and Triassic 'Karoo-like' sequences of the Congo Basin. In: de Wit, M.J., Guillocheau, F., and de Wit, M.J.C. (Eds.), *The Geology and Resource Potential of the Congo Basin*, Springer-Verlag, in press.

Linol, B., de Wit, M.J., Barton, E., Guillocheau, F., de Wit, M.J.C, and Colin. J.-P., 2014b. Chapter 8: Facies analysis, chronostratigraphy, and paleo-environmental reconstructions of the Jurassic to Cretaceous sequences of the Congo Basin. In: de Wit, M.J., Guillocheau, F., and de Wit, M.J.C. (Eds.), *The Geology and Resource Potential of the Congo Basin*, Springer-Verlag, in press.

Linol, B., de Wit, M.J., Guillocheau, F., Robin, C. and Dauteuil, O., 2014c. Chapter 11: Multiphase Phanerozoic subsidence and uplift history recorded in the Congo Basin – a complex successor basin. In: de Wit, M.J., Guillocheau, F., and de

1 Wit, M.J.C. (Eds.), The Geology and Resource Potential of the Congo Basin,
2 Springer-Verlag, in press.

3 Linol, B., de Wit, M.J., Milani, E.J., Guillocheau, F. and Scherer, C. 2014d.
4 Chapter 13: New regional correlations between the Congo, Paraná and Cape-Karoo
5 Basins of southwest Gondwana. In: de Wit, M.J., Guillocheau, F., and de Wit, M.J.C.
6 (Eds.), The Geology and Resource Potential of the Congo Basin, Springer-Verlag, in
7 press.
8

9 Lombard, A.L., 1961. La série de la Haute Lueki (partie orientale de la cuvette
10 congolaise). Bulletin de la Société belge de Géologie, de Paléontologie et
11 d'Hydrologie, 70, p.65-72.

12 Ludwig, K.R., 2003. Isoplot/version 3.0: A geochronological toolkit for Microsoft
13 Excel. Berkeley Geochronology Center Special Publication, 4, 71p.

14 Maheshwari, H., Bose, M.N., and Kumaran, K.P., 1977. Mesozoic *spora*
15 *dispersae* from Zaire. II: The Loia and Bokungu Groups in the Samba borehole. III:
16 Some miospores from the Stanleyville Group. Annales du Musée Royal de l'Afrique
17 centrale, Tervuren (Belgique), Série in-8, Sciences géologiques, 80, 60p.

18 Marlière, R., 1950. Ostracodes et phyllopoies du système du Karoo au Congo
19 Belge. Annales du Musée du Congo belge, 6, p.1-43.

20 Master, S., Rainaud, C., Armstrong, R., Phillips, D., and Robb, L., 2005.
21 Provenance ages of the Neoproterozoic Katanga Supergroup (Central African
22 Copperbelt), with implications for basin evolution. Journal of African Earth Sciences,
23 42(1-5), p.41-60.

24 Milani, E.J., and de Wit, M.J., 2008. Correlations between the classic Paraná and
25 Cape Karoo sequences of South America and southern Africa and their basin infills
26 flanking the Gondwanides: du Toit revisited. In: Pankurst, R.J., Trouw, R.A.J., Brito
27 Neves, B.B., and de Wit, M.J. (eds.), West Gondwana: Pre-Cenozoic Correlations
28 Across the South Atlantic Region. Geological Society of London, Special
29 Publications, 294, pp.319-342.

30 Milani, E.J., Gonçalves de Melo, J.H., de Souza, P.A., Fernandes, L.A., and
31 França, A.B., 2007. Bacia do Pa-raná. Boletim de geociências da petrobras, 15 (2),
32 pp.265-287.

33 Miller, R., 2008. The Geology of Namibia, Volume 3: upper Palaeozoic-Cenozoic.
34 Windhoek, Namibia: Geological Survey.

35
36
37
38
39
40
41
42
43
44
45
46
47
48
49
50
51
52
53
54
55
56
57
58
59
60
61
62
63
64
65

1
2
3
4
5
6
7
8
9
10
11
12
13
14
15
16
17
18
19
20
21
22
23
24
25
26
27
28
29
30
31
32
33
34
35
36
37
38
39
40
41
42
43
44
45
46
47
48
49
50
51
52
53
54
55
56
57
58
59
60
61
62
63
64
65

Munizaga, F., MaksaeV, V., Fanning, C.M., Giglio, S., Yaxley, G., and Tassinari, C.C.G., 2008. Late Paleozoic-Early Triassic magmatism on the western margin of Gondwana: Collahuasi area, Northern Chile. *Gondwana Research*, 13(3), p.407-427.

Nkoumbou, C., Barbey, P., Yonta-Ngouné, C., Paquette, J.L., and Villiéras, F., 2013. Pre-collisional geodynamic context of the southern margin of the Pan-African fold belt in Cameroon. *Journal of African Earth Sciences*, <http://dx.doi.org/10.1016/j.jafrearsci.2013.10.002>.

Pedrosa-Soares, A.C., Alkmim, F.F., Tack, L., Noce, C.M., Babinski, M., Silva, L.C., and Martins-Neto, M.A., 2008, Similarities and differences between the Brazilian and African counterparts of the Neoproterozoic Araçuaí-West Congo orogen. *Geological Society, London, Special Publications*, 294(1), p.153-172.

Poidevin, J.L., 1985. Le Proterozoïque supérieur de la République Centrafricaine. *Annales du Musée Royal de l'Afrique centrale, Tervuren (Belgique), Serie in-8, Sciences Géologiques*, 91, 75p.

Polinard, E., 1932. Découverte des gisements fossilifères d'eau douce sur les versants de la Lubudi au Katanga méridional. *Annales de la Société Géologique de Belgique*, 55, p.63-81.

Rainaud, C., Master, S., Armstrong, R.A. and Robb, L.J., 2003. A cryptic Mesoarchaean terrane in the basement to the Central African Copperbelt. *Journal of the Geological Society of London*, 160, p.11-14.

Ramos, V.A., and Aleman, A., 2000. Tectonic Evolution of the Andes. In: Cordani, U.G., Milani, E.J., Thomaz Filho, A., and Campos, D.A. (eds.), *Tectonic Evolution of South America*. Rio de Janeiro, Brazil: 31st international geological congress, p.635-685.

Rankin, W., Webb, S.J., Kiyani, D., Kinnaird, J.A., Jones, A.G. and Evans, R.L. (2013). Linking the Damara (Namibia) and Lufilian/Katangan (Zambia) belts through geophysical interpretations. *Proceedings of the 13th SAGA Biennial Conference and Exhibition, Kruger Park, South African Geophysical Association*, 4 pp.

Reeves, C.V., 1999. Aeromagnetic and gravity features of Gondwana and their relation to continental break-up: more pieces, less puzzle. *Journal of African Earth Sciences*, 28, p.263-277.

Robert, M., 1946. *Le Congo physique*. Troisième édition. Liège: H. Vaillant-Carmagne, 449pp.

1
2
3
4
5
6
7
8
9
10
11
12
13
14
15
16
17
18
19
20
21
22
23
24
25
26
27
28
29
30
31
32
33
34
35
36
37
38
39
40
41
42
43
44
45
46
47
48
49
50
51
52
53
54
55
56
57
58
59
60
61
62
63
64
65

Rocha-Campos, A.C., Basei, M.A., Nutman, A.P., Kleiman, L.E., Varela, R., Llambias, E., Canile, F.M., and da Rosa, O.D.C.R., 2011. 30 million years of Permian volcanism recorded in the Choiyoi igneous province (W Argentina) and the source for younger ash fall deposits in the Paraná Basin: SHRIMP U-Pb zircon geochronology evidence. *Gondwana Research*, 19(2), p.509-523.

Rolin, P., 1995. Carte tectonique de la République centrafricaine, au 1:1.500.000. BRGM.

Sachse, V.F., Delvaux, D. and Littke, R., 2012. Petrological and geochemical investigations of potential source rocks of the central Congo Basin, DRC. *American Association of Petroleum Geologists Bulletin*, 96(2), p.245-275.

Saint Seine, P., 1953. Poissons de la cuvette congolaise. *Compte rendus de la Société géologique de France*, 16, p.343-345.

Saint Seine, P., 1955. Poissons fossiles de l'étage de Stanleyville (Congo belge). 1^{ère} partie: La faune des argilites et schistes bitumineux. *Annales du Musée Royal de l'Afrique centrale, Tervuren (Belgique), Série in 8, Sciences Géologiques*, 14, 126p.

Saint Seine, P., and Casier, E., 1962. Poissons fossiles des couches de Stanleyville (Congo). 2^{ème} partie: La faune marine des calcaires de Songa. *Annales du Musée Royal de l'Afrique centrale, Tervuren (Belgique), Série in 8, Sciences Géologiques*, 44, 52p.

Simonetti, A., Heaman, L.M., Hartlaub, R.P., Creaser, R.A., MacHattie, T.G., Böhm, C., 2005. U-Pb zircon dating by laser ablation-MC-ICP-MS using a new multiple ion counting Faraday collector array. *Journal of Analytical Atomic Spectrometry*, 20, p.677-686.

Sláma, J., Košler, J., Condon, D.J., Crowley, J.L., Gerdes, A., Hanchar, J.M., Horstwood, M.S.A., Morris, G.A., Nasdala, L., Norberg, N., Schaltegger, U., Schoene, B., Tubrett, M.N., and Whitehouse, M.J., 2008. Plešovice zircon – A new natural reference material for U-Pb and Hf isotopic microanalysis. *Chemical Geology*, 249, p.1-35.

Sommer, H., Kröner, A., Hauzenberger, C., Muhongo, S., and Wingate, M.T.D., 2003. Metamorphic petrology and zircon geochronology of high-grade rocks from the central Mozambique Belt of Tanzania: crustal recycling of Archean and Palaeoproterozoic material during the Pan-African orogeny. *Journal of Metamorphic Geology*, 21, p.915-934.

1 Tack, L., Wingate, M.T.D., and Lie, J., 2001. Early Neoproterozoic magmatism
2 (1000-910 Ma) of the Zadinian and Mayumbian Groups (Bas-Congo): onset of
3 Rodinia rifting at the western edge of the Congo craton. *Precambrian Research*, 110,
4 p.277-306.
5
6

7 Tack, L., Wingate, M.T.D., de Waele, B., Meert, J., Belousova, E., Griffin, B.,
8 Tahon, A., and Fernandez-Alonso, M., 2010. The 1375 Ma “Kibaran event” in
9 Central Africa: Prominent emplacement of bimodal magmatism under extensional
10 regime. *Precambrian Research*, 180(1-2), p.63-84.
11
12

13 Tankard, A., Welsink, H., Aukes, P., Newton, R. and Stattker, E., 2012. Chapter
14 23: Geodynamic interpretation of the Cape and Karoo basins, South Africa. In:
15 Roberts, D.G. and Bally, A.W. (Eds.). *Phanerozoic Passive Margins, Cratonic Basins
16 and Global Tectonics Maps*. Amsterdam: Elsevier. pp.869-945.
17
18

19 Tait, J., Delpomdor, F., Preat, A., Tack, L., Straathof, G., and Nkula, V.K., 2011.
20 Neoproterozoic sequences of the West Congo and Lindi/Ubangi Supergroups in the
21 Congo Craton, Central Africa. In: Arnaud, E., Halverson, G.P., and Shields-Zhou, G.
22 (eds.), *The Geological Record of Neoproterozoic Glaciations*. Geological Society of
23 London, *Memoirs*, 36, pp.185-194.
24
25

26 Toteu, S.F., Van Schmus, W.R., Penaye, J., and Michard, A., 2001. New U-Pb and
27 Sm-Nd data from north-central Cameroon and its bearing on the pre-Pan African
28 history of central Africa. *Precambrian Research*, 108(1-2), p.45-73.
29
30

31 Toteu, S.F., Fouateu, R.Y., Penaye, J., Tchakounte, J., Mouangue, A.C.S., van
32 Schmus, W.R., Deloule, E., and Stendal, H., 2006. U-Pb dating of plutonic rocks
33 involved in the nappe tectonic in southern Cameroon: consequence for the Pan-
34 African orogenic evolution of the central African fold belt. *Journal of African Earth
35 Sciences*, 44(4-5), p.479-493.
36
37

38 Taverne, L., 1975, Etude ostéologique de *Leptolepis caheni*, Téléostéen fossile du
39 Jurassique supérieur (Kimmeridgien) de Kisangani (ex-Stanleyville, Zaïre)
40 précédemment décrit dans le genre *Paraclupavus*. *Revue Zoologique Africaine*, 89,
41 p.821-853.
42
43

44 Taverne, L., 1976, Les téléostéens fossiles du crétaé moyen de Kipala (Kwango,
45 Zaïre). *Annales du Musée Royal de l’Afrique centrale, Tervuren (Belgique), Série in-
46 8, Sciences géologiques*, 79, 50p.
47
48

49 Torsvik, T.H., van der Voo, R., Preeden, U., Mac Niocaill, C., Steinberger, B.,
50 Doubrovine, P.V., van Hinsbergen, D.J.J., Domeier, M., Gaina, C., Tohver, E., Meert,
51
52
53
54
55
56
57
58
59
60
61
62
63
64
65

1 J.G., McCausland, P.J.A., and Cocks, L.R., 2012. Phanerozoic Polar Wander,
2 Palaeogeography and Dynamics. *Earth Science Reviews*, 114 (3-4), p.325-368.

3 Trouw, R.A., and de Wit, M.J., 1999. Relation between the Gondwanide Orogen
4 and contemporaneous intracratonic deformation. *Journal of African Earth Sciences*,
5 28(1), p.203-213.
6

7
8
9 Zeffass, H., Chemale, F., Schultz, C.L., and Lavina, E., 2004. Tectonics and
10 sedimentation in southern South America during the Triassic. *Sedimentary Geology*,
11 166(3-4), p.265-292.
12
13
14
15
16
17
18
19
20
21
22
23
24
25
26
27
28
29
30
31
32
33
34
35
36
37
38
39
40
41
42
43
44
45
46
47
48
49
50
51
52
53
54
55
56
57
58
59
60
61
62
63
64
65

Figures

1
2 Figure 1: (A) Tectonic map of the Precambrian basement of central Gondwana (inset
3 for location) showing the Central African Shield (dotted line), and (B) main
4 Phanerozoic sequences of central Africa, with location of the field study area and the
5 four deep boreholes in the CB (updated from de Wit et al., 1988, 2008, and de Wit
6 and Linol, 2014). Red outline marks the watershed of the modern CB drainage
7 system.
8
9

10
11
12
13
14
15 Figure 2: Borehole litho- and bio-stratigraphic correlations across the central CB (Fig.
16 1B for location), showing the location of core-samples with dated detrital zircons
17 (simplified from Linol, 2013, and Linol et al., 2014a). U1, U2 and U3 mark major
18 unconformities determined from analysis of seismic.
19
20
21
22

23
24 Figure 3: Photos of outcrops along the Kwango River, southwest DRC (Fig. 1B for
25 location), showing the location of samples. (A) Cliff of red sandstones near
26 Swamasangu; cross-bed sets up to 10 m thick are characteristic of Jurassic-Cretaceous
27 aeolian dune deposits. Paleocurrent measurements (n: 49) indicate predominant paleo-
28 winds blowing to the southwest and to the south (Linol, 2013; see also Linol et al.,
29 2014b). (B) Locally mined gravels at Kitsaku infill an irregular erosion surface
30 (dotted line) incised into Karoo (late Paleozoic) conglomerates and red siltstones.
31
32
33
34
35
36
37

38
39 Figure 4: Microphotographs of selected zircons collected from the Kwango field
40 study area (WP103; Fig. 3B), and from the Samba (S) and Dekese (D) cores; sample
41 numbers refer to depth below surface (see Fig. 2).
42
43
44

45
46 Figure 5: Examples of backscatter electron microprobe images (left), Concordia
47 diagrams (middle) and frequency plots (right) of U-Pb dated detrital zircons from
48 main Phanerozoic groups of the CB (Figs. 2 and 3 for samples location). Numbers of
49 zircon with a distinct age-range are plotted at the top of the frequency plots.
50
51
52
53

54
55 Figure 6: (A) Frequency plot of all U-Pb single zircon dates from the CB, and (B)
56 simplified map of Precambrian basement ages (modified from Linol, 2013 and de Wit
57 and Linol, 2014), with main sediment dispersal directions.
58
59
60
61
62
63
64
65

1
2
3
4
5
6
7
8
9
10
11
12
13
14
15
16
17
18
19
20
21
22
23
24
25
26
27
28
29
30
31
32
33
34
35
36
37
38
39
40
41
42
43
44
45
46
47
48
49
50
51
52
53
54
55
56
57
58
59
60
61
62
63
64
65

Figure 7: Paleo-reconstructions (left; modified from Scotese, 2014) and schematic diagrams (right) showing the paleogeography and paleo-topographic evolution of the CB in central Gondwana. (A) Upper Neoproterozoic-lower Paleozoic Redbeds (in dark red) were regionally deposited southward between the Pan African Mountains surrounding the CB. (B) Carboniferous-Permian glacial and deglaciation sequences (in dark grey) derived from west-facing paleo-valleys incised along the eastern margin of the basin. These sequences possibly connected with the Karoo and Paraná Seas of southwestern Gondwana. (C) Triassic fluvial (aeolian?) red sandstones and siltstones (in brown) were deposited across the entire CB; but outcrops are poorly described. (D) Upper Jurassic-Lower Cretaceous fluvial-delta and aeolian sequences (in pink and pale red respectively) record a short marine transgression (from the proto-Indian Ocean) in the northeastern CB, and a paleo-desert in the southern part of the basin extending to Namibia and South America. Strong wind systems were blowing to the southwest at low latitudes across interior Gondwana. (E) Mid- Upper Cretaceous lake sequences (in green) and Cenozoic alluviums (in yellow) derived from the south, possibly related to marginal uplifts of the CB and the Kalahari epeirogeny of southern Africa.

Figure 8: Cross-section across western Gondwana (Fig. 7D for location) showing a Central Gondwana Basin flanked along its southern convergent margin by the proto-Andes. Prevailing near-surface paleo-wind directions were to the south, whilst delicate Permian-Jurassic detrital zircons originating from volcanoes along the proto-Andes imply high atmospheric flow regimes to the north into the interior of Gondwana (arrows).

Tables

Table 1: U-Pb results of detrital zircons from sample D1853 (the Inkisi Group).

Table 2: U-Pb results of detrital zircons from sample D1595 (the Lower Lukuga Group).

Table 3: U-Pb results of detrital zircons from sample D1400 (the Upper Lukuga Group).

1
2
3
4
5
6
7
8
9
10
11
12
13
14
15
16
17
18
19
20
21
22
23
24
25
26
27
28
29
30
31
32
33
34
35
36
37
38
39
40
41
42
43
44
45
46
47
48
49
50
51
52
53
54
55
56
57
58
59
60
61
62
63
64
65

Table 4: U-Pb results of detrital zircons from sample S2035 (the Haute Lueki Group).

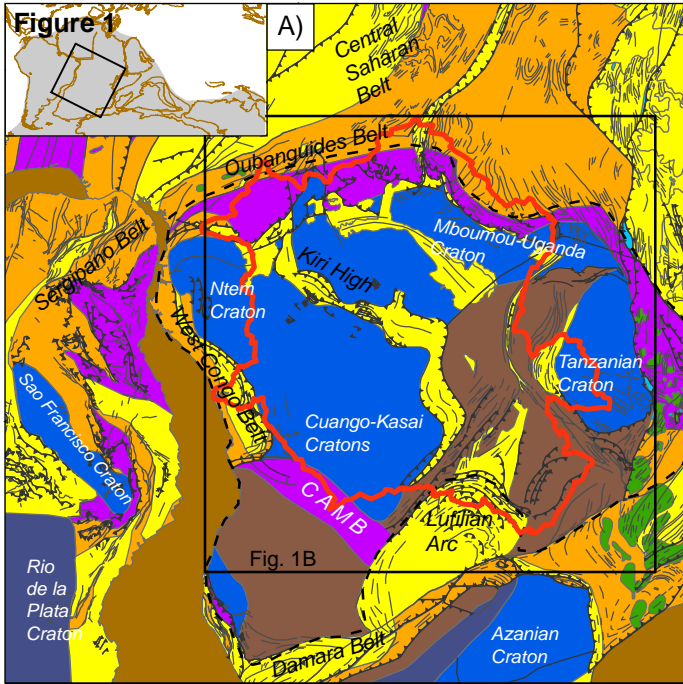
Table 5: U-Pb results of detrital zircons from sample S1605 (the Haute Lueki Group).

Table 6: U-Pb results of detrital zircons from sample D600 (the Lower Kwango Group).

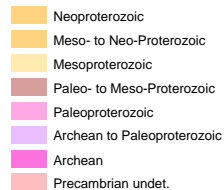
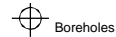
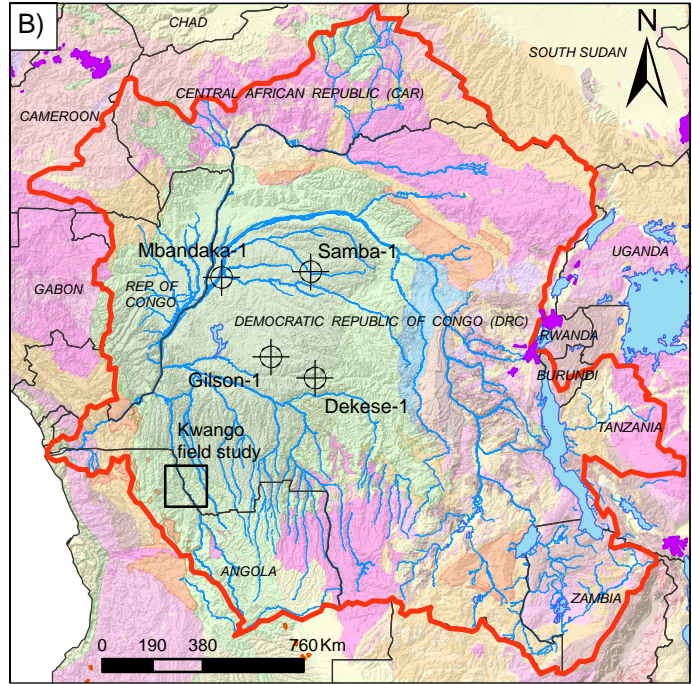
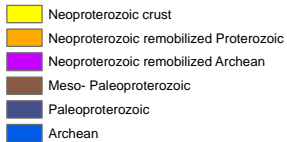
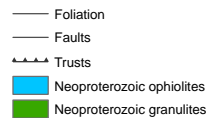
Table 7: U-Pb results of detrital zircons from sample D470 (the Lower Kwango Group).

Table 8: U-Pb results of detrital zircons from sample WP19 (the Lower Kwango Group).

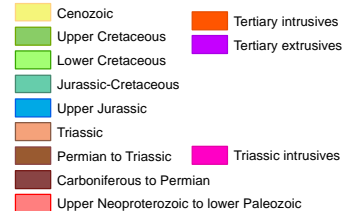
Table 9: U-Pb results of detrital zircons from sample WP103 (the Kalahari Group).

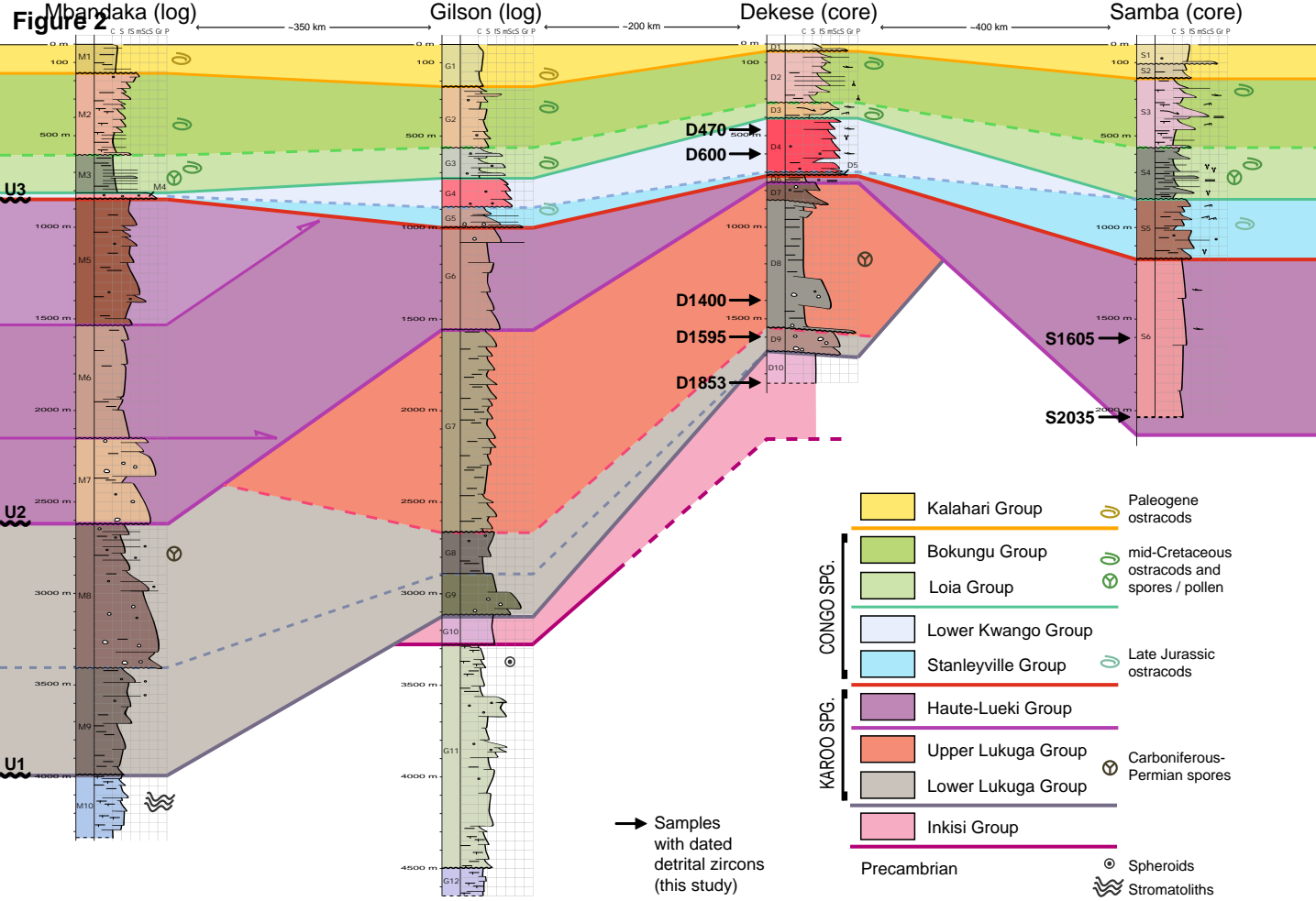


Precambrian basement:



Phanerozoic sequences:







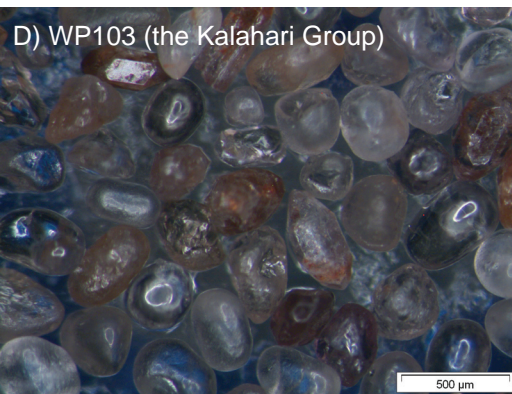
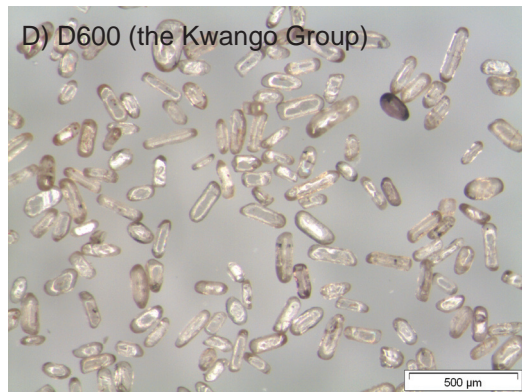
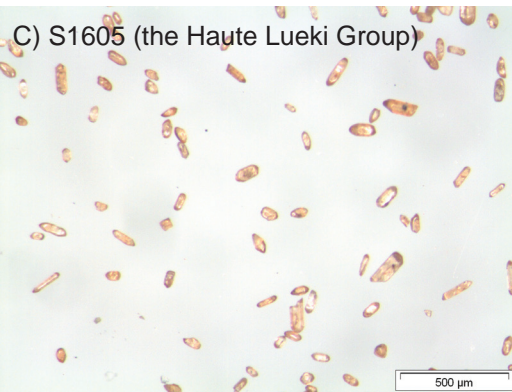
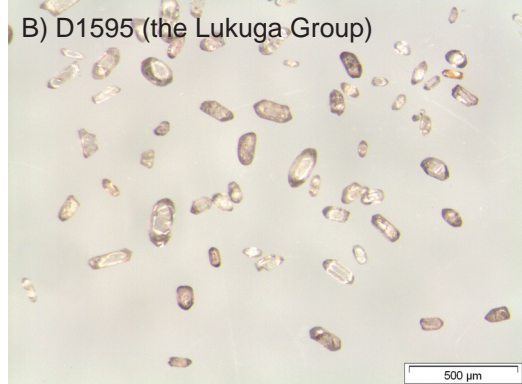
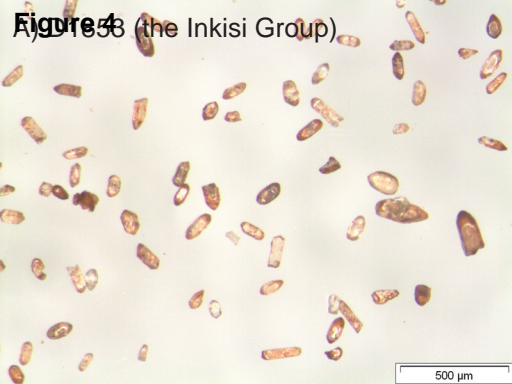
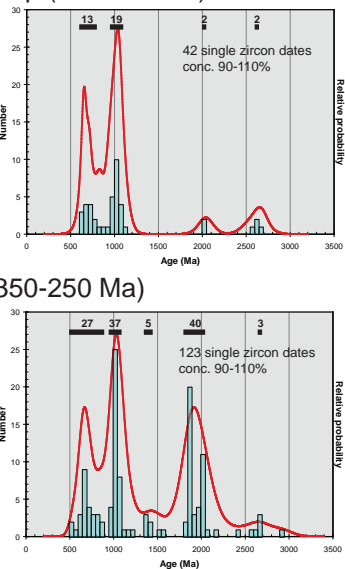
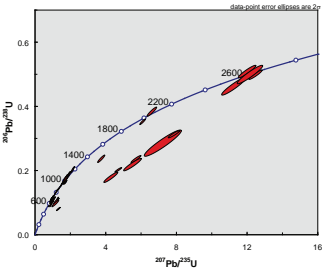
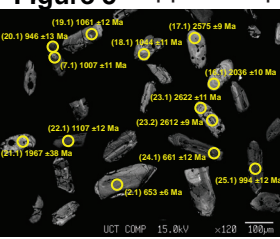
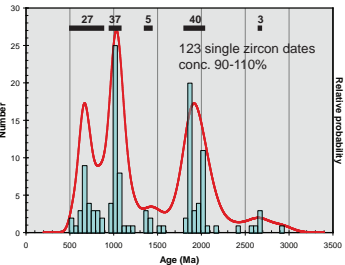
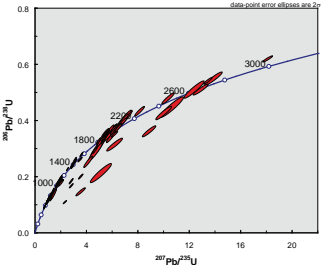
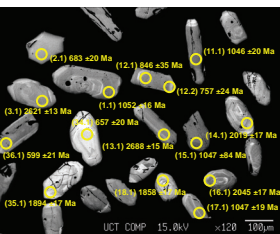


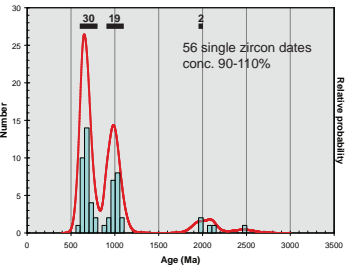
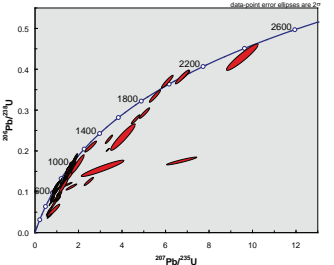
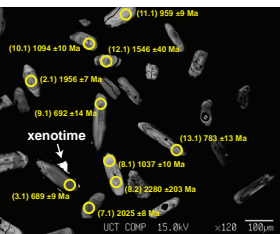
Figure 5: upper Neoproterozoic-lower Paleozoic Inksik Group (550-450 Ma)



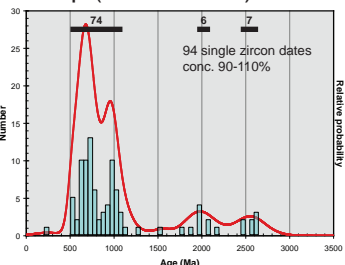
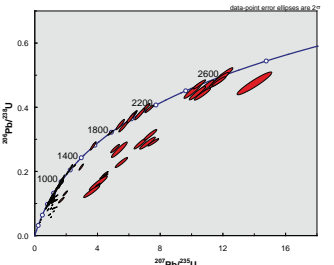
B) D1400-D1595: Carboniferous-Permian Lukuga Group (350-250 Ma)



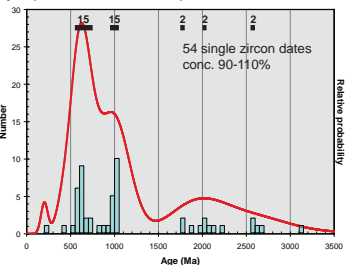
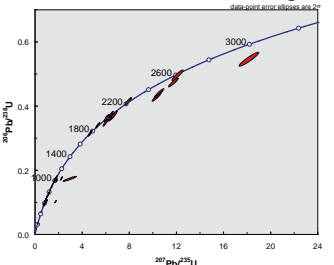
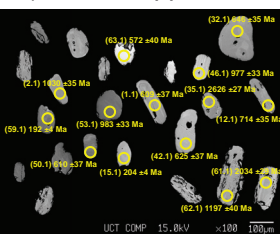
C) S1605-S2035: Triassic Haute Lueki Group (250-200 Ma)



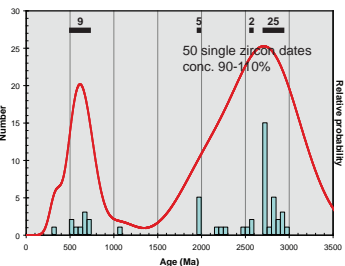
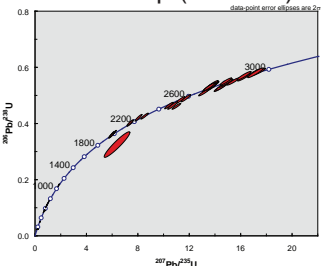
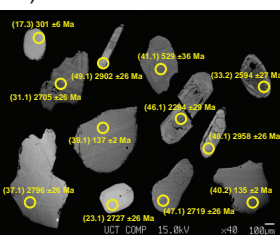
D) D470-D600: Upper Jurassic-Lower Cretaceous Kwango Group (150-100 Ma)



E) WP19: Upper Jurassic-Lower Cretaceous Kwango Group (150-100 Ma)



F) WP103: The Cenozoic Kalahari Group (70-0 Ma)



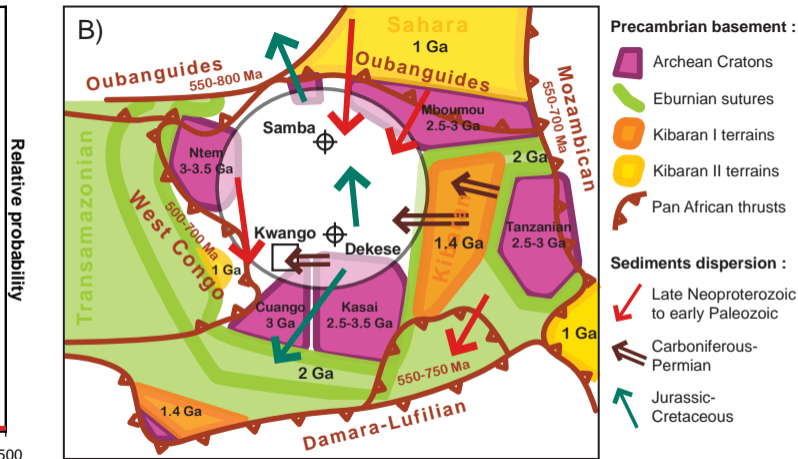
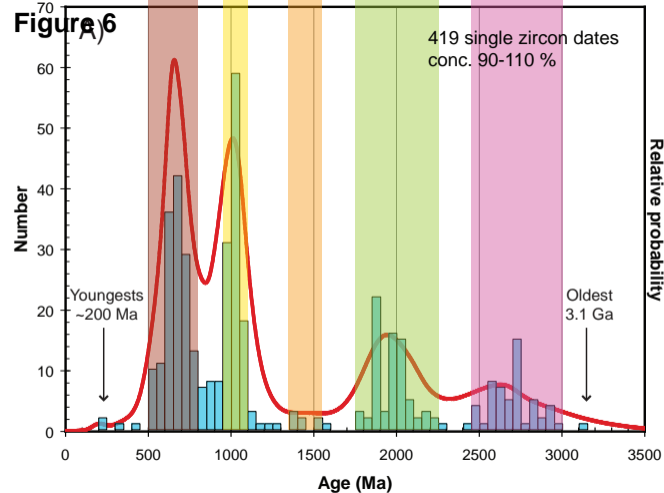
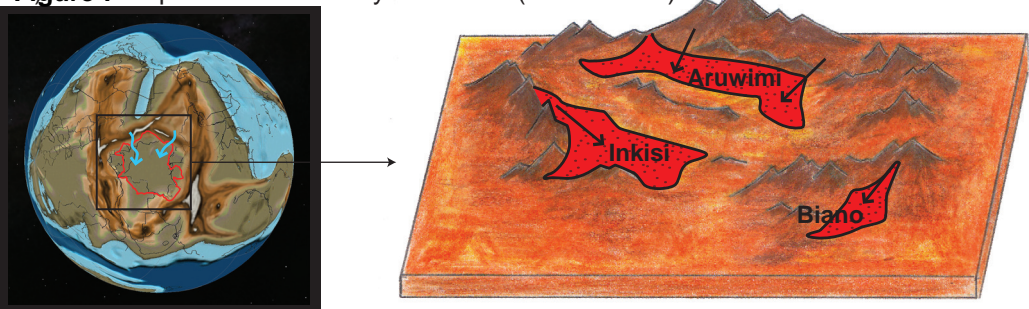
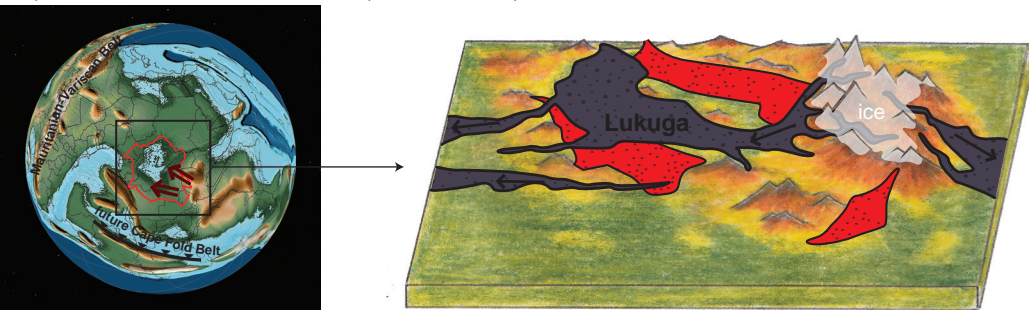


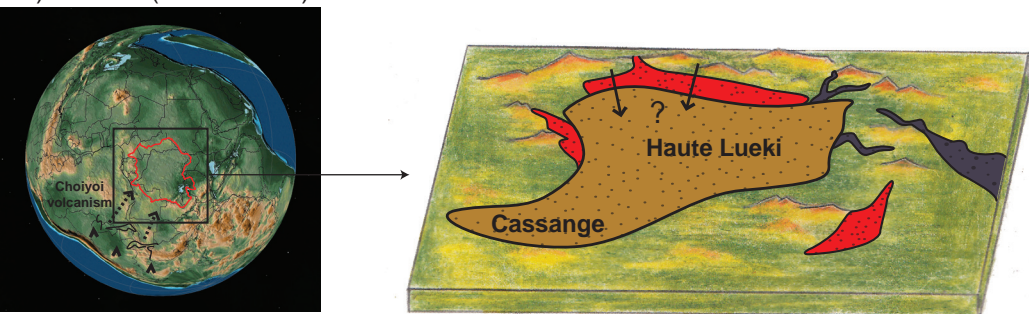
Figure 7 Neoproterozoic to early Paleozoic (550-450 Ma)



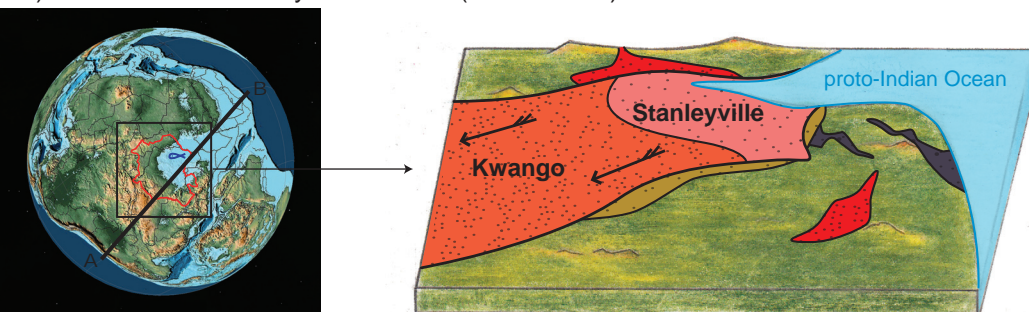
B) Carboniferous to Permian (350-300 Ma)



C) Triassic (250-200 Ma)



D) Late Jurassic to Early Cretaceous (150-100 Ma)



E) Mid-Cretaceous to Cenozoic (100-0 Ma)

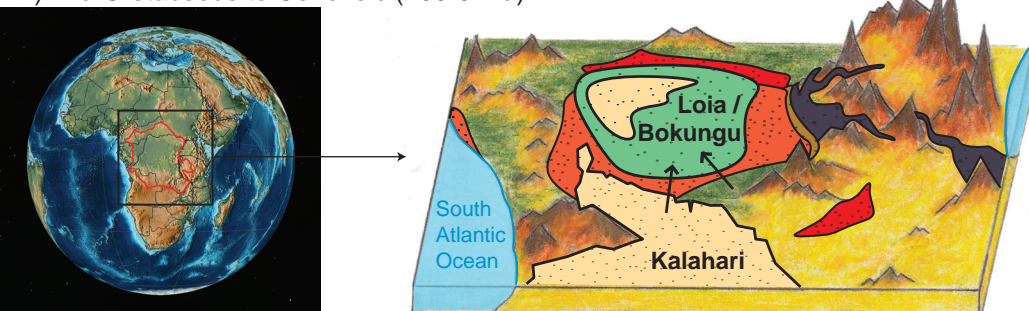


Figure 8

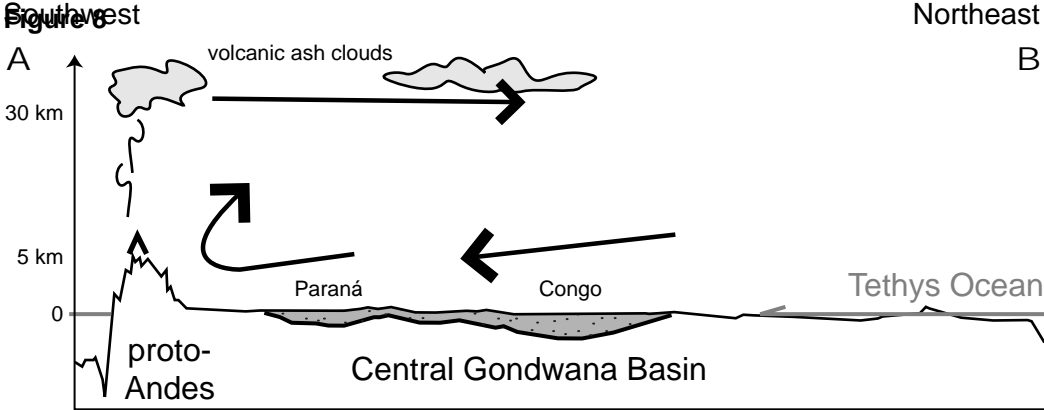


Table 1

sample	spot Ø	U [ppm]	Pb [ppm]	ratios		1σ	207Pb/235U	1σ	206Pb/238U	1σ	207Pb/206Pb	2σ	207Pb/235U	2σ	206Pb/238U	2σ	conc.
				207Pb/206Pb	207Pb/235U												
D11_L_1.1_10-35-55	35	2	0	0.083489	3.96	1.195708	5.18	0.10387	3.33	1281	77	799	58	637	41	50	
D11_L_2.1_10-35-55	35	288	27	0.061395	0.29	0.929508	1.17	0.10980	1.14	653	6	667	12	672	14	103	
D11_L_3.1_10-35-55	35	217	34	0.074285	0.31	1.834944	0.83	0.17915	0.77	1049	6	1058	11	1062	15	101	
D11_L_4.1_10-35-55	35	240	77	0.125846	0.40	6.093347	1.09	0.35117	1.01	2041	7	1989	19	1940	34	95	
D11_L_5.1_10-35-55	35	167	15	0.061223	0.37	0.853262	0.93	0.10108	0.85	647	8	626	9	621	10	96	
D11_L_6.1_10-35-55	35	204	25	0.066915	0.37	1.271852	1.01	0.13785	0.93	835	8	833	11	833	15	100	
D11_L_7.1_10-35-55	35	405	42	0.063040	0.32	1.025571	0.99	0.11799	0.94	710	7	717	10	719	13	101	
D11_L_8.1_10-35-55	35	269	41	0.074121	0.31	1.747181	0.91	0.17096	0.86	1045	6	1026	12	1017	16	97	
D11_L_9.1_10-35-55	35	826	120	0.075064	0.44	1.666577	1.20	0.16103	1.12	1070	9	996	15	962	20	90	
D11_L_10.1_10-35-55	35	796	62	0.064085	1.15	0.773519	1.38	0.08754	0.77	744	24	582	12	541	8	73	
D11_L_11.1_10-35-55	35	151	77	0.181952	0.29	12.490581	1.24	0.49788	1.21	2671	5	2642	23	2605	52	98	
D11_L_12.1_10-25-55	25	195	29	0.073562	0.56	1.760987	1.82	0.17362	1.73	1029	11	1031	24	1032	33	100	
D11_L_13.1_10-25-55	25	43	18	0.176928	0.56	11.267724	2.50	0.46189	2.44	2624	9	2546	47	2448	100	93	
D11_L_14.1_10-25-55	25	490	98	0.115437	1.00	3.748952	2.22	0.23554	1.98	1887	18	1582	36	1363	49	72	
D11_L_15.1_10-25-55	25	821	115	0.076937	0.81	1.725214	1.69	0.16263	1.48	1120	16	1018	22	971	27	87	
D11_L_16.1_10-25-55	25	493	168	0.125527	0.59	6.618316	1.67	0.38239	1.57	2036	10	2062	30	2087	56	103	
D11_L_17.1_10-25-55	25	263	125	0.171726	0.51	12.013340	1.67	0.50737	1.59	2575	9	2605	32	2645	69	103	
D11_L_18.1_10-25-55	25	440	68	0.074093	0.56	1.850553	1.73	0.18114	1.63	1044	11	1064	23	1073	32	103	
D11_L_19.1_10-25-55	25	186	29	0.074721	0.59	1.914965	2.29	0.18587	2.21	1061	12	1086	31	1099	45	104	
D11_L_20.1_10-25-55	25	56	8	0.070600	0.62	1.676111	1.73	0.17219	1.62	946	13	1000	22	1024	31	108	
D11_L_20.2_10-25-55	25	335	48	0.072755	0.56	1.691224	1.61	0.16859	1.51	1007	11	1005	21	1004	28	100	
D11_L_21.1_10-25-55	25	1110	77	0.120742	2.13	1.311818	3.39	0.07880	2.64	1967	38	851	39	489	25	25	
D11_L_22.1_10-25-55	25	58	10	0.076438	0.60	2.124907	1.98	0.20162	1.89	1107	12	1157	28	1184	41	107	
D11_L_23.1_10-25-55	25	1098	245	0.176695	0.66	5.706987	2.02	0.23425	1.91	2622	11	1932	35	1357	47	52	
D11_L_23.2_10-25-55	25	1819	299	0.175645	0.56	4.295603	3.74	0.17737	3.70	2612	9	1693	63	1053	72	40	
D11_L_24.1_10-25-55	25	191	18	0.061629	0.58	0.934118	1.82	0.10993	1.72	661	12	670	18	672	22	102	
D11_L_25.1_10-25-55	25	86	13	0.072303	0.58	1.736777	2.11	0.17421	2.03	994	12	1022	27	1035	39	104	
D11_L_26.1_10-25-55	25	572	48	0.068612	4.40	0.940815	4.86	0.09945	2.07	887	91	673	48	611	24	69	
D11_L_27.1_10-25-55	25	288	45	0.072089	0.53	1.763349	2.13	0.17741	2.06	988	11	1032	28	1053	40	107	
D11_L_28.1_10-25-55	25	584	54	0.070794	0.84	1.068269	2.94	0.10944	2.82	951	17	738	31	670	36	70	
D11_L_29.1_10-25-55	25	360	34	0.063939	1.79	0.966155	2.51	0.10959	1.75	740	38	686	25	670	22	91	
D11_L_30.1_10-25-55	25	1708	454	0.184534	0.61	7.235245	5.93	0.28436	5.89	2694	10	2141	109	1613	169	60	
D11_S_1.1_10-25-55	25	291	28	0.062530	0.61	0.961700	1.54	0.11155	1.42	692	13	684	15	682	18	98	
D11_S_2.1_10-25-55	25	290	42	0.070956	0.64	1.606576	1.73	0.16422	1.60	956	13	973	22	980	29	103	
D11_S_3.1_10-25-55	25	190	28	0.074328	1.10	1.710133	2.21	0.16687	1.92	1050	22	1012	29	995	35	95	
D11_S_4.1_10-25-55	25	259	24	0.060671	0.58	0.896927	1.89	0.10722	1.80	628	13	650	18	657	23	105	
D11_S_5.1_10-25-55	25	343	42	0.068411	0.97	1.343863	1.73	0.14247	1.43	881	20	865	20	859	23	97	
D11_S_6.1_10-25-55	25	70	11	0.074227	0.73	1.829605	1.82	0.17877	1.67	1048	15	1056	24	1060	33	101	
D11_S_7.1_10-25-55	25	502	51	0.062955	0.71	1.009572	1.63	0.11631	1.47	707	15	709	17	709	20	100	
D11_S_8.1_10-25-55	25	198	22	0.065017	0.56	1.127694	1.77	0.12580	1.67	775	12	767	19	764	24	99	
D11_S_9.1_10-25-55	25	491	70	0.073629	0.86	1.644191	1.72	0.16196	1.49	1031	17	987	22	968	27	94	
D11_S_10.1_10-25-55	25	119	11	0.065225	1.03	0.940255	1.73	0.10455	1.40	782	22	673	17	641	17	82	
D11_S_11.1_10-25-55	25	311	30	0.061755	0.71	0.924913	1.61	0.10862	1.45	666	15	665	16	665	18	100	
D11_S_12.1_10-25-55	25	104	16	0.074319	0.87	1.756150	2.03	0.17138	1.83	1050	17	1029	26	1020	35	97	
D11_S_13.1_10-25-55	25	90	8	0.060140	0.97	0.893960	2.56	0.10781	2.37	609	21	648	25	660	30	108	
D11_S_14.1_10-25-55	25	219	32	0.070785	0.57	1.642160	1.94	0.16826	1.85	951	12	987	25	1003	34	105	
D11_S_15.1_10-25-55	25	52	8	0.073656	0.75	1.896507	1.99	0.18674	1.84	1032	15	1080	27	1104	37	107	
D11_S_16.1_10-25-55	25	371	57	0.073437	0.61	1.762692	1.64	0.17409	1.53	1026	12	1032	21	1035	29	101	
D11_S_17.1_10-25-55	25	621	49	0.071136	1.44	0.924739	4.07	0.09428	3.81	961	29	665	40	581	42	60	
D11_S_18.1_10-25-55	25	175	28	0.074311	0.76	1.812840	1.76	0.17693	1.59	1050	15	1050	23	1050	31	100	
D11_S_19.1_10-25-55	25	967	200	0.184456	0.61	5.516352	3.66	0.21690	3.61	2693	10	1903	64	1265	83	47	
D11_S_20.1_10-25-55	25	419	33	0.086354	5.23	1.145617	6.84	0.09622	4.41	1346	101	775	76	592	50	44	
D11_S_21.1_10-25-55	25	534	49	0.069455	0.77	0.987241	1.68	0.10309	1.50	912	16	697	17	632	18	69	
D11_S_22.1_10-25-55	25	431	38	0.066068	1.59	0.910583	2.29	0.09996	1.65	809	33	657	22	614	19	76	
D11_S_23.1_10-25-55	25	482	147	0.182898	0.78	7.865586	1.65	0.31190	1.46	2679	13	2216	30	1750	45	65	
D11_S_24.1_10-25-55	25	516	50	0.066339	1.33	1.007969	2.67	0.11020	2.32	817	28	708	27	674	30	82	
D11_S_25.1_10-25-55	25	542	55	0.082468	0.76	1.271270	1.52	0.11180	1.32	1257	15	833	17	683	17	54	
D11_S_26.1_10-25-55	25	122	17	0.070250	0.65	1.500763	1.79	0.15494	1.67	936	13	931	22	929	29	99	
D11_S_27.1_10-25-55	25	596	59	0.063871	0.96	0.983693	1.88	0.11170	1.62	737	20	695	19	683	21	93	
D11_S_28.1_10-25-55	25	44	7	0.072340	0.65	1.723921	2.90	0.17284	2.83	996	13	1017	38	1028	54	103	
D11_S_29.1_10-25-55	25	355	41	0.065575	0.70	1.200736	1.82	0.13280	1.68	793	15	801	20	804	25	101	
D11_S_30.1_10-25-55	25	178	86	0.177166	0.59	12.171414	2.42	0.49826	2.35	2627	10	2618	46	2606	101	99	
D11_S_30.2_10-25-55	25	616	121	0.170312	0.77	4.711967	1.68	0.20066	1.49	2561	13	1769	28	1179	32	46	

Table 4

sample	spot Ø	U [ppm]	Pb [ppm]	ratios $^{207}\text{Pb}/^{206}\text{Pb}$	$^{207}\text{Pb}/^{235}\text{U}$			$^{206}\text{Pb}/^{238}\text{U}$			$^{207}\text{Pb}/^{206}\text{Pb}$			$^{207}\text{Pb}/^{235}\text{U}$			$^{206}\text{Pb}/^{238}\text{U}$			conc.
					1σ	1σ	1σ	1σ	1σ	1σ	2σ	2σ	2σ	2σ	2σ	2σ	2σ	2σ		
S10 L 1.1 10-25-55	25	1548	92	0.090611	1.27	0.876986	6.26	0.07020	6.13	1438	24	639	60	437	52	30				
S10 L 1.2 10-25-55	25	1054	149	0.076974	1.60	1.774952	2.39	0.16724	1.78	1121	32	1036	31	997	33	89				
S10 L 2.1 10-25-55	25	491	143	0.120003	0.40	5.511502	1.85	0.33310	1.81	1956	7	1902	32	1853	58	95				
S10 L 3.1 10-25-55	25	329	31	0.062427	0.43	0.958710	1.39	0.11138	1.33	689	9	683	14	681	17	99				
S10 L 3.2 10-20-55	25	61	11	0.280890	3.58	6.749587	4.22	0.17428	2.24	3368	56	2079	76	1036	43	31				
S10 L 4.1 10-25-55	25	1399	110	0.081118	0.44	1.029034	1.60	0.09200	1.53	1224	9	718	17	567	17	46				
S10 L 5.1 10-25-55	25	295	56	0.088777	3.40	2.567568	4.27	0.20976	2.58	1399	65	1291	63	1228	58	88				
S10 L 6.1 10-25-55	25	1197	84	0.066324	0.72	0.756089	1.86	0.08268	1.72	817	15	572	16	512	17	63				
S10 L 7.1 10-25-55	25	170	25	0.073387	0.41	1.745827	1.59	0.17254	1.53	1025	8	1026	21	1026	29	100				
S10 L 8.1 10-25-55	25	1167	156	0.073844	0.48	1.571251	1.59	0.15432	1.52	1037	10	959	20	925	26	89				
S10 L 8.2 10-20-55	25	1321	174	0.144330	11.78	3.111394	12.88	0.15635	5.20	2280	203	1436	208	936	91	41				
S10 L 9.1 10-25-55	25	604	54	0.062509	0.65	0.925015	1.62	0.10733	1.48	692	14	665	16	657	19	95				
S10 L 10.1 10-25-55	25	611	94	0.075954	0.49	1.875213	1.46	0.17906	1.38	1094	10	1072	19	1062	27	97				
S10 L 11.1 10-25-55	25	874	123	0.071042	0.46	1.586280	2.27	0.16194	2.22	959	9	965	28	968	40	101				
S10 L 12.1 10-25-55	25	1656	117	0.095904	2.12	1.071488	3.72	0.08103	3.06	1546	40	739	39	502	30	32				
S10 L 13.1 10-25-55	25	913	79	0.065281	0.61	0.916682	1.59	0.10184	1.47	783	13	661	16	625	18	80				
S10 L 14.1 10-25-55	25	734	103	0.071039	0.38	1.617237	1.43	0.16511	1.37	959	8	977	18	985	25	103				
S10 L 15.1 10-25-55	25	602	81	0.070386	0.45	1.512715	1.20	0.15587	1.12	940	9	936	15	934	19	99				
S10 L 16.1 10-25-55	25	296	43	0.072672	1.30	1.678859	1.79	0.16755	1.23	1005	26	1001	23	999	23	99				
S10 L 16.2 10-25-55	25	627	127	0.108310	0.86	3.397139	2.06	0.22748	1.87	1771	16	1504	33	1321	45	75				
S10 L 17.1 10-25-55	25	1669	122	0.069036	0.73	0.826738	2.27	0.08685	2.15	900	15	612	21	537	22	60				
S10 L 18.1 10-25-55	25	881	73	0.064348	0.38	0.859518	1.29	0.09688	1.23	753	8	630	12	596	14	79				
S10 L 18.2 10-20-55	25	2542	94	0.114913	7.32	0.842923	13.98	0.05320	11.91	1879	132	621	134	334	78	18				
S10 L 19.1 10-25-55	25	709	62	0.065639	1.71	0.921313	2.79	0.10180	2.20	795	36	663	27	625	26	79				
S10 L 19.2 10-25-55	25	469	40	0.063097	0.65	0.846206	1.69	0.09727	1.56	711	14	623	16	598	18	84				
S10 L 20.1 10-25-55	25	839	110	0.070880	0.57	1.472928	1.44	0.15072	1.32	954	12	919	18	905	22	95				
S10 L 21.1 10-25-55	25	829	109	0.071597	0.58	1.519822	3.07	0.15396	3.02	974	12	938	38	923	52	95				
S10 L 22.1 10-25-55	25	959	65	0.073163	1.81	0.797571	4.68	0.07906	4.32	1018	37	595	43	491	41	48				
S10 L 23.1 10-25-55	25	2521	86	0.122222	2.56	0.640217	5.28	0.03799	4.62	1989	46	502	42	240	22	12				
S10 S_1.1_10-25-55	25	1465	153	0.077599	0.62	1.307860	2.31	0.12224	2.23	1137	12	849	27	743	31	65				
S10 S_2.1_10-25-55	25	382	37	0.063415	0.61	0.997329	2.05	0.11406	1.95	722	13	702	21	696	26	96				
S10 S_3.1_10-25-55	25	687	52	0.067563	1.38	0.851736	4.24	0.09143	4.01	855	29	626	40	564	43	66				
S10 S_4.1_10-25-55	25	215	33	0.073490	0.58	1.768238	2.11	0.17451	2.03	1027	12	1034	28	1037	39	101				
S10 S_5.1_10-25-55	25	1328	172	0.074902	0.73	1.575857	1.88	0.15259	1.74	1066	15	961	24	915	30	86				
S10 S_6.1_10-25-55	25	411	63	0.073127	0.62	1.810898	1.76	0.17960	1.65	1017	13	1049	23	1065	32	105				
S10 S_7.1_10-25-55	25	3252	121	0.123776	1.25	0.708929	3.34	0.04154	3.09	2011	22	544	28	262	16	13				
S10 S_8.1_10-25-55	25	1468	393	0.125244	0.64	5.042121	1.91	0.29198	1.80	2032	11	1826	33	1651	52	81				
S10 S_8.2_10-25-55	25	611	213	0.129270	0.61	6.781080	1.93	0.38045	1.83	2088	11	2083	34	2078	65	100				
S10 S_9.1_10-25-55	25	432	68	0.072965	0.57	1.854578	1.88	0.18434	1.79	1013	12	1065	25	1091	36	108				
S10 S_10.1_10-25-55	25	254	23	0.061148	0.65	0.931817	1.81	0.11052	1.68	644	14	669	18	676	22	105				
S10 S_10.2_10-25-55	25	115	11	0.061634	0.69	0.935554	1.80	0.11009	1.66	661	15	671	18	673	21	102				
S10 S_11.1_10-25-55	25	726	68	0.061017	0.58	0.930760	1.69	0.11063	1.59	640	12	668	17	676	20	106				
S10 S_11.2_10-25-55	25	345	35	0.064390	1.13	1.041561	1.96	0.11732	1.60	754	24	725	20	715	22	95				
S10 S_12.1_10-25-55	25	900	86	0.062873	1.07	0.966889	1.96	0.11153	1.65	704	23	687	20	682	21	97				
S10 S_13.1_10-25-55	25	245	25	0.062538	0.73	1.011906	1.95	0.11735	1.81	693	16	710	20	715	25	103				
S10 S_13.2_10-20-55	20	197	20	0.109656	5.32	1.673722	5.97	0.11070	2.71	1794	97	999	77	677	35	38				
S10 S_13.3_10-20-55	20	148	17	0.144426	1.05	2.472503	3.44	0.12416	3.28	2281	18	1264	50	754	47	33				
S10 S_14.1_10-25-55	25	1098	97	0.083662	0.74	1.179860	1.82	0.10228	1.66	1285	14	791	20	628	20	49				
S10 S_14.2_10-25-55	25	1178	106	0.083602	0.85	1.302320	6.60	0.11298	6.55	1283	17	847	77	690	86	54				
S10 S_15.1_10-25-55	25	2195	91	0.092630	4.14	0.611942	6.91	0.04791	5.54	1480	78	485	54	302	33	20				
S10 S_16.1_10-25-55	25	217	20	0.060884	0.65	0.919799	1.96	0.10957	1.85	635	14	662	19	670	24	106				
S10 S_17.1_10-25-55	25	983	72	0.068889	2.10	0.844468	4.58	0.08891	4.07	895	43	622	43	549	43	61				
S10 S_18.1_10-25-55	25	626	89	0.072618	0.64	1.647216	2.04	0.16452	1.93	1003	13	988	26	982	35	98				
S10 S_19.1_10-25-55	25	405	31	0.087143	4.28	1.036429	5.27	0.08626	3.08	1364	82	722	55	533	32	39				
S10 S_20.1_10-25-55	25	1233	111	0.062056	0.81	0.893284	1.86	0.10440	1.68	676	17	648	18	640	20	95				
S10 S_21.1_10-25-55	25	177	28	0.073464	0.71	1.857454	1.84	0.18337	1.70	1027	14	1066	24	1085	34	106				
S10 S_22.1_10-25-55	25	172	18	0.064096	0.88	1.049461	2.28	0.11875	2.10	745	19	729	24	723	29	97				
S10 S_23.1_10-25-55	25	477	47	0.062681	0.62	1.001469	1.88	0.11588	1.77	697	13	705	19	707	24	101				
S10 S_23.2_10-25-55	25	562	55	0.064192	0.80	0.985258	1.87	0.11132	1.69	748	17	696	19	680	22	91				
S10 S_24.1_10-25-55	25	401	38	0.061341	0.61	0.941076	1.79	0.11127	1.69	651	13	673	18	680	22	104				

Table 5

sample	spot Ø	U [ppm]	Pb [ppm]	ratios		1σ	²⁰⁷ Pb/ ²³⁵ U	1σ	²⁰⁶ Pb/ ²³⁸ U	1σ	²⁰⁷ Pb/ ²⁰⁶ Pb	2σ	²⁰⁷ Pb/ ²³⁵ U	2σ	²⁰⁶ Pb/ ²³⁸ U	2σ	conc.
				²⁰⁷ Pb/ ²⁰⁶ Pb	1σ												
S8 L_1.1_10-35-55	35	731	63	0.062131	0.30	0.882789	0.83	0.10305	0.78	679	6	642	8	632	9	93	
S8 L_1.2_10-35-55	35	308	28	0.060269	0.67	0.875916	1.94	0.10541	1.82	613	14	639	18	646	22	105	
S8 L_2.1_10-35-55	35	955	129	0.080402	0.63	1.778234	2.15	0.16041	2.06	1207	12	1038	28	959	37	79	
S8 L_3.1_10-35-55	35	272	25	0.065632	0.86	1.005293	1.60	0.11109	1.35	795	18	706	16	679	17	85	
S8 L_4.1_10-35-55	35	353	64	0.120373	0.39	3.342706	0.83	0.20140	0.74	1962	7	1491	13	1183	16	60	
S8 L_4.2_10-25-55	25	509	202	0.161342	0.58	9.542483	3.13	0.42896	3.07	2470	10	2392	58	2301	120	93	
S8 L_5.1_10-35-55	35	314	27	0.062969	0.40	0.885584	1.01	0.10200	0.93	707	8	644	10	626	11	89	
S8 L_6.1_10-35-55	35	321	28	0.064164	0.47	0.897184	1.21	0.10141	1.12	747	10	650	12	623	13	83	
S8 L_7.1_10-35-55	35	224	32	0.072794	0.40	1.673689	0.88	0.16675	0.78	1008	8	999	11	994	14	99	
S8 L_8.1_10-35-55	35	181	64	0.130352	0.29	6.938641	1.05	0.38606	1.01	2103	5	2104	19	2105	36	100	
S8 L_9.1_10-35-55	35	525	71	0.069021	0.28	1.471451	0.89	0.15462	0.84	899	6	919	11	927	15	103	
S8 L_10.1_10-35-55	35	119	11	0.060762	0.34	0.866531	1.20	0.10343	1.15	631	7	634	11	634	14	101	
S8 L_11.1_10-25-55	25	216	19	0.060244	0.72	0.857201	1.76	0.10320	1.61	612	16	629	17	633	19	103	
S8 L_12.1_10-25-55	25	249	24	0.061554	0.63	0.945108	1.89	0.11136	1.78	659	14	676	19	681	23	103	
S8 L_13.1_10-25-55	25	451	41	0.064369	0.81	0.944863	2.36	0.10646	2.22	754	17	675	23	652	28	87	
S8 L_14.1_10-25-55	25	1721	77	0.090818	2.27	0.688446	6.84	0.05498	6.45	1443	43	532	57	345	43	24	
S8 L_15.1_10-25-55	25	231	20	0.059324	0.65	0.833028	2.21	0.10184	2.11	579	14	615	20	625	25	108	
S8 L_16.1_10-25-55	25	768	93	0.083269	1.28	1.678712	4.90	0.14621	4.73	1276	25	1000	63	880	78	69	
S8 L_16.2_10-25-55	25	1496	104	0.089042	1.45	1.066583	6.30	0.08688	6.13	1405	28	737	67	537	63	38	
S8 L_17.1_10-25-55	25	164	15	0.061290	0.65	0.888874	1.82	0.10518	1.70	649	14	646	17	645	21	99	
S8 L_107.1_10-35-55	35	450	53	0.072019	0.68	1.339644	1.91	0.13491	1.78	986	14	863	22	816	27	83	
S8 L_18.1_10-35-55	35	837	72	0.072242	0.79	0.996260	2.01	0.10002	1.85	993	16	702	20	615	22	62	
S8 L_19.1_10-35-55	35	100	10	0.073592	1.98	1.098952	2.59	0.10830	1.67	1030	40	753	28	663	21	64	
S8 L_20.1_10-35-55	35	82	8	0.071990	2.56	1.060979	3.13	0.10689	1.80	986	52	734	33	655	22	66	
S8 L_21.1_10-35-55	35	599	51	0.061037	0.76	0.826210	1.82	0.09817	1.66	641	16	612	17	604	19	94	
S8 L_22.1_10-35-55	35	239	22	0.061822	0.67	0.895715	1.71	0.10508	1.57	668	14	649	16	644	19	96	
S8 L_23.1_10-35-55	35	787	77	0.079767	0.59	1.222759	1.76	0.11118	1.65	1191	12	811	20	680	21	57	
S8 L_24.1_10-35-55	35	308	45	0.071891	0.61	1.654017	1.73	0.16687	1.62	983	12	991	22	995	30	101	
S8 L_25.1_10-35-55	35	316	33	0.093328	4.85	1.504712	5.15	0.11693	1.73	1495	92	932	64	713	23	48	
S8 L_26.1_10-35-55	35	522	39	0.068184	2.41	0.825132	4.41	0.08777	3.69	874	50	611	41	542	38	62	
S8 L_27.1_10-35-55	35	251	22	0.060531	0.70	0.856346	1.81	0.10260	1.68	623	15	628	17	630	20	101	
S8 L_28.1_10-35-55	35	140	15	0.065624	0.77	1.092754	1.76	0.12077	1.58	794	16	750	19	735	22	93	
S8 L_29.1_10-35-55	35	401	29	0.067829	0.86	0.764344	3.16	0.08173	3.04	863	18	577	28	506	30	59	
S8 L_30.1_10-35-55	35	645	42	0.074644	1.95	0.762653	2.99	0.07410	2.27	1059	39	576	26	461	20	44	
S8 S_1.1_10-25-55	25	227	19	0.060622	0.60	0.835128	1.60	0.09991	1.48	626	13	616	15	614	17	98	
S8 S_2.1_10-25-55	25	879	51	0.072128	0.63	0.684402	2.36	0.06882	2.27	990	13	529	20	429	19	43	
S8 S_3.1_10-25-55	25	431	106	0.121372	0.64	4.630761	1.75	0.27671	1.63	1976	11	1755	29	1575	46	80	
S8 S_4.1_10-25-55	25	159	22	0.072275	0.59	1.653470	1.56	0.16592	1.44	994	12	991	20	990	26	100	
S8 S_5.1_10-25-55	25	1070	71	0.085696	5.04	0.930227	5.55	0.07873	2.32	1331	98	668	55	489	22	37	
S8 S_6.1_10-25-55	25	963	189	0.125981	0.62	4.049742	5.72	0.23314	5.68	2043	11	1644	95	1351	139	66	
S8 S_7.1_10-25-55	25	635	68	0.079441	0.85	1.391955	2.62	0.12708	2.48	1183	17	886	31	771	36	65	
S8 S_8.1_10-25-55	25	438	57	0.070980	0.69	1.490233	1.64	0.15227	1.49	957	14	926	20	914	25	95	
S8 S_9.1_10-25-55	25	3112	112	0.101990	0.90	0.573965	2.32	0.04082	2.14	1661	17	461	17	258	11	16	
S8 S_9.2_10-15-55	15	1087	128	0.077588	3.00	1.539294	4.23	0.14389	2.97	1136	60	946	53	867	48	76	
S8 S_10.1_10-25-55	25	782	87	0.075327	0.65	1.344778	1.63	0.12948	1.50	1077	13	865	19	785	22	73	
S8 S_11.1_10-25-55	25	314	40	0.070580	0.61	1.428753	1.60	0.14682	1.48	945	12	901	19	883	24	93	
S8 S_12.1_10-25-55	25	814	60	0.065359	0.90	0.775091	1.86	0.08601	1.63	786	19	583	17	532	17	68	
S8 S_13.1_10-25-55	25	305	26	0.062963	0.87	0.872620	1.64	0.10052	1.40	707	18	637	16	617	16	87	
S8 S_14.1_10-25-55	25	789	73	0.062687	0.72	0.945276	1.87	0.10937	1.73	698	15	676	19	669	22	96	
S8 S_15.1_10-25-55	25	716	91	0.073712	0.75	1.513933	1.99	0.14896	1.84	1034	15	936	24	895	31	87	
S8 S_16.1_10-25-55	25	188	20	0.068033	0.70	1.179764	1.95	0.12577	1.81	870	15	791	21	764	26	88	
S8 S_17.1_10-25-55	25	196	18	0.062193	0.73	0.930300	1.72	0.10849	1.56	681	16	668	17	664	20	98	
S8 S_18.1_10-25-55	25	622	66	0.080118	3.41	1.346519	4.24	0.12189	2.53	1200	67	866	50	741	36	62	
S8 S_19.1_10-25-55	25	46	5	0.073197	1.71	1.209594	2.64	0.11985	2.00	1019	35	805	30	730	28	72	
S8 S_20.1_10-20-55	20	429	38	0.061621	0.66	0.883360	2.03	0.10397	1.93	661	14	643	19	638	23	96	
S8 S_21.1_10-25-55	20	924	67	0.068055	0.82	0.792204	1.95	0.08443	1.77	870	17	592	18	522	18	60	
S8 S_21.2_10-20-55	20	365	34	0.061893	0.76	0.902427	2.13	0.10575	1.99	670	16	653	21	648	25	97	
S8 S_22.1_10-20-55	20	278	90	0.119734	0.60	6.092328	1.78	0.36903	1.68	1952	11	1989	31	2025	58	104	
S8 S_23.1_10-20-55	20	291	42	0.085556	2.39	1.968137	6.10	0.16684	5.61	1328	46	1105	84	995	104	75	
S8 S_24.1_10-20-55	20	156	21	0.076693	0.98	1.598027	2.61	0.15112	2.42	1113	20	969	33	907	41	81	
S8 S_25.1_10-20-55	20	306	46	0.074724	0.65	1.796955	2.04	0.17441	1.93	1061	13	1044	27	1036	37	98	
S8 S_26.1_10-20-55	20	222	19	0.061334	0.70	0.842129	1.79	0.09958	1.64	651	15	620	17	612	19	94	
S8 S_27.1_10-20-55	20	265	25	0.063415	0.96	0.934459	2.27	0.10687	2.06	722	20	670	22	655	26	91	
S8 S_28.1_10-20-55	20	430	51	0.077857	0.74	1.441718	2.01	0.13430	1.87	1143	15	906	24	812	29	71	

Table 7

sample	spot Ø	U [ppm]	Pb [ppm]	ratios ²⁰⁷ Pb/ ²⁰⁶ Pb	ratios						conc.					
					1σ	²⁰⁷ Pb/ ²³⁵ U	1σ	²⁰⁶ Pb/ ²³⁸ U	1σ	²⁰⁷ Pb/ ²⁰⁶ Pb		2σ	²⁰⁷ Pb/ ²³⁵ U	2σ	²⁰⁶ Pb/ ²³⁸ U	2σ
D470L_1.1_10-35-55	35	69	10	0.074645	1.52	1.676141	1.70	0.16286	0.76	1059	31	1000	22	973	14	92
D470L_2.1_10-35-55	35	110	11	0.064408	1.25	1.034282	1.53	0.11647	0.88	755	26	721	16	710	12	94
D470L_3.1_10-35-55	35	193	17	0.061740	1.20	0.891279	1.42	0.10470	0.76	665	26	647	14	642	9	97
D470L_4.1_10-35-55	35	132	38	0.109322	1.18	4.793333	1.50	0.31800	0.92	1788	22	1784	25	1780	29	100
D470L_5.1_10-35-55	35	298	24	0.059941	1.22	0.773851	1.55	0.09363	0.96	601	26	582	14	577	11	96
D470L_6.1_10-35-55	35	175	17	0.063249	1.20	0.994829	1.41	0.11408	0.74	717	25	701	14	696	10	97
D470L_8.1_10-35-55	35	355	67	0.083116	1.18	2.467578	1.38	0.21532	0.72	1272	23	1263	20	1257	17	99
D470L_9.1_10-35-55	35	168	15	0.077424	1.73	1.075048	1.94	0.10070	0.88	1132	34	741	21	619	10	55
D470L_10.1_10-35-55	35	63	6	0.063110	1.41	0.950408	1.69	0.10922	0.94	712	30	678	17	668	12	94
D470L_11.1_10-35-55	35	119	18	0.071908	1.24	1.694605	1.43	0.17092	0.73	983	25	1007	18	1017	14	103
D470L_12.1_10-35-55	35	91	8	0.061668	1.34	0.839793	1.54	0.09877	0.76	663	29	619	14	607	9	92
D470L_13.1_10-35-55	35	185	18	0.063250	1.32	0.966748	1.52	0.11085	0.75	717	28	687	15	678	10	95
D470L_14.1_10-35-55	35	89	8	0.064214	2.34	0.895174	2.50	0.10111	0.91	749	49	649	24	621	11	83
D470L_15.1_10-35-55	35	58	5	0.060362	1.40	0.780138	1.59	0.09374	0.76	617	30	586	14	578	8	94
D470L_16.1_10-35-55	35	49	4	0.061430	1.58	0.783012	1.75	0.09245	0.75	654	34	587	16	570	8	87
D470L_17.2_10-25-55	25	63	2	0.051011	5.57	0.266404	5.73	0.03788	1.37	241	128	240	25	240	6	99
D470L_18.1_10-35-55	35	516	41	0.058301	0.95	0.756842	1.53	0.09415	1.20	541	21	572	13	580	13	107
D470L_19.1_10-35-55	35	920	88	0.062573	0.97	0.988991	1.62	0.11463	1.30	694	21	698	16	700	17	101
D470L_20.1_10-35-55	35	590	22	0.052825	1.11	0.330436	1.63	0.04537	1.19	321	25	290	8	286	7	89
D470L_21.1_10-35-55	35	132	44	0.120527	0.93	6.245480	1.62	0.37582	1.32	1964	17	2011	28	2057	47	105
D470L_22.1_10-35-55	35	464	38	0.058651	0.94	0.793745	1.56	0.09815	1.24	554	21	593	14	604	14	109
D470L_23.1_10-35-55	35	148	12	0.061570	1.07	0.835682	1.69	0.09844	1.31	659	23	617	16	605	15	92
D470L_24.1_10-35-55	35	387	35	0.060115	1.00	0.903274	1.63	0.10898	1.29	608	22	653	16	667	16	110
D470L_25.1_10-35-55	35	667	69	0.063409	0.94	1.074665	1.63	0.12292	1.33	722	20	741	17	747	19	104
D470L_26.1_10-35-55	35	278	23	0.058601	1.02	0.805872	1.61	0.09974	1.25	552	22	600	15	613	15	111
D470L_27.1_10-35-55	35	252	37	0.071664	0.95	1.704956	1.75	0.17255	1.47	976	19	1010	23	1026	28	105
D470L_28.1_10-35-55	35	108	10	0.062111	1.07	0.908769	1.68	0.10612	1.30	678	23	656	16	650	16	96
D470L_29.1_10-35-55	35	155	16	0.063496	0.96	1.080800	1.77	0.12345	1.49	725	20	744	19	750	21	104
D470L_30.1_10-35-55	35	372	34	0.081658	1.13	1.194011	1.74	0.10605	1.32	1237	22	798	19	650	16	53
D470L_31.1_10-35-55	35	204	26	0.068513	0.94	1.409045	1.55	0.14916	1.23	884	19	893	18	896	21	101
D470L_32.1_10-35-55	35	1881	327	0.174933	0.94	4.418893	1.79	0.18321	1.52	2605	16	1716	30	1084	30	42
D470L_32.2_10-35-55	35	1905	340	0.169889	0.94	4.440462	1.88	0.18957	1.63	2557	16	1720	31	1119	34	44
D470L_33.1_10-35-55	35	75	11	0.069328	1.04	1.612438	1.68	0.16868	1.32	909	21	975	21	1005	25	111
D470L_34.1_10-35-55	35	121	20	0.075988	0.98	2.019754	1.58	0.19277	1.23	1095	20	1122	22	1136	26	104
D470L_35.1_10-35-55	35	187	63	0.121210	0.94	6.221460	1.57	0.37227	1.26	1974	17	2007	28	2040	44	103
D470L_36.1_10-35-55	35	503	46	0.061647	0.96	0.895812	1.53	0.10539	1.20	662	21	649	15	646	15	98
D470L_37.1_10-35-55	35	20	2	0.079614	2.44	1.325250	2.73	0.12073	1.23	1187	48	857	32	735	17	62
D470L_38.1_10-35-55	35	240	24	0.064847	0.96	1.043370	1.56	0.11669	1.23	769	20	726	16	712	17	92
D470L_39.1_10-35-55	35	1690	257	0.181116	1.24	4.012798	5.85	0.16069	5.72	2663	21	1637	97	961	103	36
D470L_40.1_10-35-55	35	1138	311	0.181336	0.95	7.160021	2.84	0.28637	2.68	2665	16	2132	51	1623	77	61
D470L_41.1_10-35-55	35	357	129	0.128682	0.95	7.054161	1.59	0.39758	1.28	2080	17	2118	29	2158	47	104
D470L_42.1_10-35-55	35	187	21	0.065373	0.99	1.156266	1.57	0.12828	1.22	786	21	780	17	778	18	99
D470L_43.1_10-35-55	35	978	75	0.057786	0.95	0.708826	1.51	0.08896	1.18	522	21	544	13	549	12	105
D470L_43.2_10-25-55	25	898	76	0.058192	0.98	0.770530	1.57	0.09603	1.23	537	22	580	14	591	14	110
D470L_44.1_10-35-55	35	1184	204	0.171420	0.94	4.285241	1.82	0.18131	1.56	2572	16	1691	30	1074	31	42
D470L_45.1_10-25-55	25	152	22	0.073863	1.87	1.641557	2.34	0.16119	1.41	1038	38	986	30	963	25	93
D470L_46.1_10-25-55	25	240	27	0.064808	1.03	1.128800	1.67	0.12632	1.31	768	22	767	18	767	19	100
D470L_47.1_10-25-55	25	138	22	0.071613	1.06	1.778317	1.89	0.18010	1.56	975	22	1038	25	1068	31	109
D470L_48.1_10-25-55	25	804	94	0.105712	1.85	1.881514	3.12	0.12909	2.51	1727	34	1075	42	783	37	45
D470S_1.1_10-35-55	35	199	16	0.060223	1.12	0.788949	1.71	0.09501	1.29	612	24	591	15	585	14	96
D470S_2.1_10-35-55	35	803	58	0.100738	3.31	1.141343	3.63	0.08217	1.50	1638	61	773	40	509	15	31
D470S_2.2_10-35-55	35	667	51	0.106870	3.49	1.245052	3.68	0.08449	1.17	1747	64	821	42	523	12	30
D470S_3.1_10-35-55	35	264	23	0.063970	1.02	0.880216	1.40	0.09980	0.96	741	22	641	13	613	11	83
D470S_4.1_10-35-55	35	451	31	0.057567	0.97	0.644660	1.36	0.08122	0.96	513	21	505	11	503	9	98
D470S_5.1_10-35-55	35	1016	195	0.099926	1.04	2.912307	2.11	0.21138	1.83	1623	19	1385	32	1236	41	76
D470S_6.1_10-35-55	35	454	41	0.069831	2.08	1.020180	2.80	0.10596	1.88	923	43	714	29	649	23	70
D470S_7.1_10-35-55	35	767	63	0.082652	0.97	1.055514	1.44	0.09262	1.06	1261	19	732	15	571	12	45
D470S_8.1_10-35-55	35	197	17	0.063480	1.31	0.895607	1.68	0.10232	1.05	724	28	649	16	628	13	87
D470S_9.1_10-35-55	35	107	10	0.063200	1.44	0.912852	1.82	0.10476	1.11	715	31	659	18	642	14	90
D470S_10.1_10-35-55	35	1247	82	0.114484	1.27	1.140602	1.65	0.07226	1.05	1872	23	773	18	450	9	24
D470S_10.2_10-35-55	35	594	63	0.070738	1.00	1.173362	1.51	0.12030	1.14	950	20	788	17	732	16	77
D470S_11.1_10-35-55	35	1271	70	0.103083	2.87	0.883199	3.49	0.06214	1.98	1680	53	643	33	389	15	23
D470S_11.2_10-35-55	35	1406	70	0.129000	1.00	0.969227	1.44	0.05449	1.03	2084	18	688	14	342	7	16
D470S_12.1_10-35-55	35	415	41	0.072654	1.89	1.141115	2.43	0.11391	1.52	1004	38	773	26	695	20	69
D470S_13.1_10-35-55	35	247	21	0.062295	1.05	0.822429	1.45	0.09575	1.00	684	22	609	13	589	11	86
D470S_14.1_10-35-55	35	61	6	0.064918	1.12	0.980616	1.54	0.10956	1.06	772	24	694	16	670	13	87
D470S_15.1_10-35-55	35	494	36	0.086289	2.18	0.966949	2.52	0.08127	1.27	1345	42	687	25	504	12	37
D470S_16.1_10-35-55	35	86	10	0.065521	1.06	1.146754	1.42	0.12694	0.93	791	22	776	15	770	14	97
D470S_17.1_10-35-55	35	218	21	0.063764	1.20	0.967378	1.61	0.11003	1.06	734	26	687	16	673	14	92
D470S_18.1_10-35-55	35	34	3	0.087947	2.88	1.302839	3.16	0.10744	1.29	1381	55	847	37	658	16	48
D470S_19.1_10-35-55	35	129	13	0.064785	1.04	1.001412	1.51	0.11211	1.09	767	22	705	15	685	14	89
D470S_20.1_10-35-55	35	434	31	0.058413	0.98	0.670045	1.41	0.08319	1.01							

Table 8

sample	spot Ø	U [ppm]	Pb [ppm]	ratios			1σ	207Pb/235U	1σ	206Pb/238U	1σ	207Pb/206Pb	2σ	207Pb/235U	2σ	206Pb/238U	2σ	conc.
				207Pb/206Pb	1σ	207Pb/206Pb												
01WP19_10-35-50	35	199	16	0.06016	0.865929	0.78501	1.366175	0.09464	1.056693	609	37	588	12	583	12	96		
02WP19_10-35-50	35	57	8	0.07360	0.863175	1.66703	1.311009	0.16427	0.98675	1030	35	996	17	980	18	95		
03WP19_10-35-50	35	393	113	0.10840	0.803599	4.67879	1.181829	0.31304	0.866573	1773	29	1763	20	1756	27	99		
04WP19_10-35-50	35	316	32	0.06326	0.813397	1.01048	1.19925	0.11586	0.881241	717	35	709	12	707	12	99		
05WP19_10-35-50	35	434	36	0.06011	0.816779	0.80276	1.285921	0.09686	0.99321	607	35	598	12	596	11	98		
06WP19_10-35-50	35	86	7	0.05978	0.866318	0.79055	1.434852	0.09592	1.143807	596	37	591	13	590	13	99		
07WP19_10-35-50	35	84	7	0.05981	0.933839	0.79489	1.40474	0.09639	1.049399	597	40	594	13	593	12	99		
08WP19_10-35-50	35	212	18	0.06150	0.831595	0.86558	1.239844	0.10208	0.9196	657	36	633	12	627	11	95		
09WP19_10-35-50	35	329	110	0.12982	0.809438	6.50536	1.533368	0.36344	1.302316	2095	28	2047	27	1998	45	95		
10WP19_10-35-50	35	526	31	0.05472	0.817479	0.51494	1.312	0.06826	1.026193	401	37	422	9	426	8	106		
11WP19_10-35-50	35	986	94	0.06196	0.805689	0.93704	1.251943	0.10968	0.958241	673	35	671	12	671	12	100		
12WP19_10-35-50	35	153	46	0.11373	0.806939	5.31475	1.325618	0.33892	1.05172	1860	29	1871	23	1881	34	101		
13WP19_10-35-50	35	266	27	0.06318	0.826036	1.02368	1.203103	0.11751	0.874713	714	35	716	12	716	12	100		
14WP19_10-35-50	35	167	24	0.07286	0.850017	1.66158	1.345499	0.16539	1.042994	1010	34	994	17	987	19	98		
15WP19_10-35-50	35	478	13	0.05138	0.857846	0.22792	1.378792	0.03217	1.07943	258	39	208	5	204	4	79		
16WP19_10-35-50	35	561	43	0.05912	0.814965	0.71797	1.292567	0.08807	1.003275	572	35	549	11	544	10	95		
16bWP19_10-35-50	35	638	49	0.05876	0.821614	0.73680	1.273838	0.09095	0.973455	558	36	561	11	561	10	101		
17WP19_10-35-50	35	135	20	0.07246	0.816963	1.68599	1.438828	0.16876	1.184398	999	33	1003	18	1005	22	101		
18WP19_10-25-50	25	697	68	0.12500	0.807802	1.74112	1.724183	0.10102	1.523241	2029	29	1024	22	620	18	31		
19WP19_10-35-50	35	52	8	0.07338	0.832473	1.74050	1.642493	0.17203	1.4159	1024	34	1024	21	1023	26	100		
20WP19_10-35-50	35	209	81	0.13879	0.802581	7.92868	1.429283	0.41432	1.182672	2212	28	2223	26	2235	45	101		
21WP19_10-35-50	35	204	31	0.07373	0.816387	1.73175	1.391995	0.17035	1.127459	1034	33	1020	18	1014	21	98		
22WP19_10-35-50	35	225	19	0.06022	0.820485	0.79858	1.419086	0.09618	1.157847	612	35	596	13	592	13	97		
23WP19_10-35-50	35	734	58	0.06477	0.841961	0.81205	1.970996	0.09094	1.782113	767	35	604	18	561	19	73		
24WP19_10-25-50	25	268	124	0.18046	0.802319	11.75646	1.407563	0.47250	1.156511	2657	27	2585	27	2495	48	94		
25WP19_10-35-50	35	265	41	0.09372	0.911798	2.23339	1.511539	0.17283	1.205559	1503	34	1192	21	1028	23	68		
26WP19_10-35-50	35	188	29	0.07408	0.813637	1.79318	1.405279	0.17556	1.145777	1044	33	1043	18	1043	22	100		
27WP19_10-35-50	35	125	13	0.06617	0.974778	1.16559	1.562145	0.17275	1.220698	812	41	785	17	775	18	95		
28WP19_10-35-50	35	194	63	0.12155	0.801961	6.05768	1.464222	0.36145	1.225073	1979	29	1984	26	1989	42	101		
29WP19_10-35-50	35	234	75	0.12510	0.835172	5.99801	1.583318	0.34775	1.345134	2030	30	1976	28	1924	45	95		
30WP19_10-35-50	35	168	68	0.17546	0.801571	10.31199	1.416244	0.42625	1.167575	2610	27	2463	26	2289	45	88		
31WP19_10-35-50	35	53	30	0.24191	0.920201	18.18887	1.861566	0.54533	1.618227	3133	29	3000	36	2806	74	90		
32WP19_10-35-50	35	231	21	0.06120	0.811635	0.88555	1.526611	0.10494	1.292977	646	35	644	15	643	16	100		
33WP19_10-35-50	35	182	28	0.07364	0.825524	1.73396	1.586966	0.17077	1.355349	1032	33	1021	21	1016	26	99		
34WP19_10-35-50	35	168	13	0.05838	0.850932	0.70624	1.670208	0.08774	1.437188	544	37	543	14	542	15	100		
35WP19_10-35-50	35	184	88	0.17715	0.801989	12.10053	1.58936	0.49542	1.372181	2626	27	2612	30	2594	59	99		
36WP19_10-50-50	50	20	2	0.06752	0.906452	1.14685	1.518602	0.12320	1.2184	854	38	776	16	749	17	88		
37WP19_10-35-50	35	22	3	0.07378	0.948847	1.74314	1.670343	0.17136	1.374677	1035	38	1025	21	1020	25	98		
38WP19_10-35-50	35	242	29	0.06741	0.810343	1.29514	1.747786	0.13934	1.54858	851	34	844	20	841	24	99		
39WP19_10-35-50	35	197	16	0.05975	0.833398	0.79772	1.601839	0.09683	1.367968	594	36	596	14	596	15	100		
40WP19_10-35-50	35	766	66	0.06036	0.805777	0.83231	1.486036	0.10001	1.24861	616	35	615	14	614	15	100		
41WP19_10-35-50	35	177	26	0.07359	0.811426	1.71513	1.70167	0.16904	1.49575	1030	33	1014	22	1007	28	98		
42WP19_10-35-50	35	100	9	0.06060	0.852781	0.85439	1.60595	0.10226	1.360823	625	37	627	15	628	16	100		
43WP19_10-50-50	50	80	10	0.06979	0.824765	1.44290	1.622053	0.14994	1.396717	922	34	907	20	901	24	98		
44WP19_10-35-50	35	156	13	0.05977	0.86716	0.79793	1.602479	0.09682	1.34758	595	38	596	14	596	15	100		
45WP19_10-35-50	35	132	11	0.06993	1.595722	0.98992	2.075339	0.10267	1.326916	926	65	699	21	630	16	68		
46WP19_10-35-50	35	232	33	0.07169	0.817325	1.60229	1.330857	0.16211	1.050314	977	33	971	17	968	19	99		
47WP19_10-35-50	35	34	10	0.10802	0.821148	4.67806	1.451443	0.31411	1.19683	1766	30	1763	24	1761	37	100		
48WP19_10-50-50	50	57	4	0.06083	0.823742	0.76664	1.297642	0.09141	1.002659	633	35	578	11	564	11	89		
49WP19_10-50-50	50	54	8	0.07403	0.828683	1.79937	1.330364	0.17629	1.040746	1042	33	1045	17	1047	20	100		
50WP19_10-35-50	35	185	16	0.06019	0.848397	0.80836	1.392829	0.09741	1.104624	610	37	602	13	599	13	98		
51WP19_10-20-50	20	370	158	0.17397	0.804633	10.46297	1.369002	0.43620	1.107579	2596	27	2477	26	2334	43	90		
52WP19_10-25-50	25	170	73	0.17394	0.809937	10.61159	1.254716	0.44247	0.958287	2596	27	2490	23	2362	38	91		
53WP19_10-50-50	50	207	29	0.07189	0.803139	1.63618	1.172923	0.16507	0.85482	983	33	984	15	985	16	100		
54WP19_10-35-50	35	176	25	0.07155	0.807583	1.61777	1.387327	0.16398	1.128046	973	33	977	17	979	21	101		
55WP19_10-35-50	35	119	40	0.13122	0.814389	6.71565	1.607758	0.37117	1.386239	2114	29	2075	29	2035	48	96		
56WP19_10-75-50	35	142	22	0.12371	7.479892	2.93663	7.700259	0.17217	1.82899	2010	265	1391	120	1024	35	51		
57WP19_10-35-50	35	170	24	0.07104	0.814846	1.57559	1.19895	0.16085	0.879492	959	33	961	15	961	16	100		
58WP19_10-35-50	50	28	2	0.06116	0.936561	0.82964	1.353106	0.09838	0.976601	645	40	613	12	605	11	94		
59WP19_10-35-50	35	474	12	0.05013	0.829301	0.20857	1.35392	0.03018	1.070215	201	38	192	5	192	4	95		
59bWP19_10-35-50	35	312	8	0.05034	0.853064	0.21212	1.333046	0.03056	1.02435	211	39	195	5	194	4	92		
60WP19_10-35-50	35	34	5	0.07317	0.903702	1.71763	1.384856	0.17026	1.049356	1019	37	1015	18	1014	19	100		
61WP19_10-35-50	35	410	142	0.12536	0.805764	6.43468	1.317229	0.37228	1.042035	2034	29	2037	23	2040	37	100		
62WP19_10-35-50	50	56	8	0.07999	1.014293	1.84577	1.381359	0.16736	0.937743	1197	40	1062	18	998	17	83		
63WP19_10-35-50	35	890	70	0.05914	0.921093	0.74810	1.263474	0.09174	0.864843	572	40	567	11	566	9	99		
64WP19_10-35-50	35	101	9	0.06062	0.859201	0.89912	1.276932	0.10757	0.944631	626	37	651	12	659	12	105		

Table 9

sample	spot Ø	U [ppm]	Pb [ppm]	ratios $^{207}\text{Pb}/^{206}\text{Pb}$	$^{207}\text{Pb}/^{235}\text{U}$			$^{206}\text{Pb}/^{238}\text{U}$			$^{207}\text{Pb}/^{206}\text{Pb}$			$^{207}\text{Pb}/^{235}\text{U}$			$^{206}\text{Pb}/^{238}\text{U}$			conc.
					1σ	2σ	3σ	1σ	2σ	3σ	1σ	2σ	3σ	1σ	2σ	3σ	1σ	2σ	3σ	
01WP103sm_10-35-50	35	63	34	0.20007	0.81	14.97042	1.22	0.54268	0.91	2827	26	2813	23	2795	41	99				
02WP103sm_10-35-50	35	594	52	0.06042	0.81	0.83539	1.27	0.10028	0.99	619	35	617	12	616	12	100				
03WP103sm_10-35-50	35	221	72	0.12113	0.81	5.93093	1.31	0.35510	1.04	1973	29	1966	23	1959	35	99				
04WP103sm_10-35-50	35	514	54	0.06378	0.81	1.05971	1.42	0.12050	1.17	734	34	734	15	733	16	100				
05WP103sm_10-35-50	35	254	39	0.07462	0.81	1.83428	1.30	0.17827	1.02	1058	33	1058	17	1058	20	100				
06WP103sm_10-35-50	35	118	60	0.18654	0.81	13.64560	1.30	0.53054	1.02	2712	27	2725	25	2744	46	101				
07WP103sm_10-35-50	35	337	33	0.06289	0.81	0.98926	1.36	0.11409	1.09	704	35	698	14	696	14	99				
08bWP103sm_10-25-50	25	63	32	0.19859	0.82	14.41919	1.35	0.52660	1.07	2815	27	2778	26	2727	47	97				
09WP103sm_10-35-50	35	570	51	0.06157	0.81	0.90457	1.20	0.10656	0.89	659	35	654	12	653	11	99				
10WP103sm_10-35-50	35	419	32	0.05871	0.82	0.72896	1.24	0.09004	0.93	557	36	556	11	556	10	100				
11WP103sm_10-35-50	35	142	62	0.16343	0.81	10.42338	1.30	0.46257	1.02	2491	27	2473	24	2451	42	98				
12WP103sm_10-35-50	35	126	63	0.18619	0.80	13.55225	1.43	0.52790	1.19	2709	27	2719	27	2733	53	101				
13WP103sm_10-35-50	35	55	28	0.18700	0.81	13.50589	1.28	0.52382	0.99	2716	27	2716	24	2715	44	100				
14bWP103sm_10-35-50	35	152	49	0.14327	2.84	6.39227	6.39	0.32360	5.73	2267	98	2031	115	1807	182	80				
14WP103sm_10-35-50	35	309	147	0.17415	0.80	11.73734	1.32	0.48880	1.05	2598	27	2584	25	2565	45	99				
15WP103sm_10-35-50	35	376	35	0.06148	0.81	0.90836	1.29	0.10716	1.01	656	35	656	13	656	13	100				
16WP103sm_10-35-50	35	95	49	0.18683	0.80	13.53936	1.33	0.52560	1.06	2714	27	2718	25	2723	47	100				
17bWP103sm_10-35-50	35	131	5	0.05416	0.92	0.35586	1.33	0.04766	0.96	378	41	309	7	300	5	79				
17cWP103sm_10-35-50	35	114	5	0.05509	0.93	0.36288	1.39	0.04778	1.03	416	41	314	7	301	6	72				
17dWP103sm_10-75-50	75	98	4	0.05538	0.81	0.37329	1.26	0.04889	0.96	427	36	322	7	308	6	72				
17eWP103sm_10-75-50	75	118	5	0.05491	0.88	0.36353	1.27	0.04802	0.92	409	39	315	7	302	5	74				
17WP103sm_10-50-50	50	67	3	0.05514	1.00	0.36915	1.36	0.04856	0.92	418	44	319	7	306	5	73				
18WP103sm_10-35-50	35	90	41	0.16996	0.85	11.29713	1.37	0.48207	1.08	2557	29	2548	26	2536	45	99				
19WP103sm_10-35-50	35	123	39	0.12189	0.80	6.13563	1.29	0.36508	1.01	1984	29	1995	23	2006	35	101				
20WP103sm_10-35-50	35	133	67	0.18686	0.80	13.71868	1.27	0.53248	0.98	2715	26	2730	24	2752	44	101				
21WP103sm_10-35-50	35	89	44	0.18794	0.81	13.66140	1.46	0.52719	1.22	2724	27	2727	28	2730	54	100				
22WP103sm_10-35-50	35	74	37	0.18708	0.81	13.54329	1.25	0.52504	0.95	2717	27	2718	24	2721	42	100				
23bWP103sm_10-25-50	25	247	131	0.18794	0.81	13.86411	1.33	0.53503	1.06	2724	27	2740	25	2763	48	101				
23WP103sm_10-25-50	25	388	203	0.18824	0.80	13.61932	1.28	0.52474	1.00	2727	26	2724	24	2719	45	100				
24bWP103sm_10-50-50	50	32	16	0.18605	0.80	13.81621	1.27	0.53860	0.98	2708	27	2737	24	2778	44	103				
24WP103sm_10-35-50	35	174	89	0.18668	0.80	13.47529	1.37	0.52352	1.11	2713	26	2714	26	2714	49	100				
25WP103sm_10-35-50	35	59	30	0.18738	0.81	13.60240	1.31	0.52649	1.03	2719	27	2722	25	2727	46	100				
26WP103sm_10-35-50	35	49	25	0.19892	0.82	14.60648	1.49	0.53256	1.24	2817	27	2790	28	2752	55	98				
27WP103sm_10-35-50	35	174	17	0.06224	0.82	0.95558	1.37	0.11135	1.09	682	35	681	14	681	14	100				
28WP103sm_10-50-50	50	32	12	0.13950	0.81	8.06304	1.42	0.41919	1.17	2221	28	2238	26	2257	45	102				
29WP103sm_10-50-50	50	111	59	0.19867	0.80	14.84285	1.31	0.54185	1.04	2815	26	2805	25	2791	48	99				
30WP103sm_10-35-50	35	141	75	0.20408	0.80	15.43298	1.25	0.54847	0.96	2859	26	2842	24	2819	44	99				
31WP103L_10-50-50	50	38	19	0.18573	0.80	13.57669	1.36	0.53017	1.09	2705	26	2721	26	2742	49	101				
32WP103L_10-75-50	75	70	5	0.06451	1.44	0.78070	1.72	0.08777	0.95	759	61	586	15	542	10	71				
33bWP103L_10-25-50	25	165	73	0.17369	0.80	11.01570	1.26	0.45997	0.96	2594	27	2524	24	2439	39	94				
33WP103L_10-75-50	35	68	30	0.16784	0.83	10.71807	1.46	0.46314	1.21	2536	28	2499	27	2453	49	97				
34WP103L_10-35-50	35	137	44	0.12125	0.81	6.02265	1.28	0.36025	0.99	1975	29	1979	22	1983	34	100				
35WP103L_10-25-50	25	74	39	0.19877	0.81	14.93828	1.23	0.54507	0.93	2816	27	2811	24	2805	42	100				
36WP103L_10-50-50	50	18	9	0.18757	0.81	13.78757	1.29	0.53312	1.01	2721	27	2735	25	2755	45	101				
37WP103L_10-50-50	50	24	13	0.19637	0.80	14.85374	1.26	0.54862	0.97	2796	26	2806	24	2819	44	101				
38WP103L_10-50-50	50	21	8	0.13451	0.81	7.38867	1.30	0.39839	1.02	2158	28	2160	23	2162	38	100				
39bWP103L_10-75-50	75	22	0	0.07473	1.30	0.22464	1.64	0.02180	0.99	1061	52	206	6	139	3	13				
39cWP103L_10-100-50	100	20	0	0.07279	1.13	0.21460	1.45	0.02138	0.90	1008	46	197	5	136	2	14				
39dWP103L_10-120-50	120	16	0	0.07187	1.11	0.20991	1.37	0.02118	0.81	982	45	193	5	135	2	14				
39eWP103L_10-120-60	0	0	0	0.07521	1.27	0.22598	1.46	0.02179	0.73	1074	51	207	5	139	2	13				
39fWP103L_10-120-70	0	0	0	0.07488	1.08	0.22734	1.29	0.02202	0.72	1065	43	208	5	140	2	13				
39WP103L_10-50-50	50	20	0	0.07623	2.12	0.22591	2.31	0.02149	0.90	1101	85	207	9	137	2	12				
40bWP103L_10-100-50	100	92	2	0.05527	0.89	0.16120	1.25	0.02115	0.88	423	40	152	4	135	2	32				
40cWP103L_10-120-50	120	48	1	0.05821	0.92	0.16929	1.22	0.02109	0.79	538	40	159	4	135	2	25				
40dWP103L_10-75-50	75	100	2	0.05518	0.89	0.16267	1.27	0.02138	0.91	420	40	153	4	136	2	32				
40eWP103L_10-75-50	75	84	1	0.05626	0.94	0.16660	1.25	0.02148	0.81	463	42	156	4	137	2	30				
40WP103L_10-50-50	50	90	2	0.05453	0.94	0.15765	1.41	0.02097	1.05	393	42	149	4	134	3	34				
41WP103L_10-35-50	35	358	25	0.05797	0.82	0.65841	1.29	0.08237	1.00	529	36	514	10	510	10	96				
42WP103L_10-35-50	35	198	64	0.12094	0.81	5.98419	1.51	0.35886	1.27	1970	29	1974	26	1977	43	100				
43WP103L_10-50-50	50	78	6	0.05833	0.85	0.69017	1.39	0.08581	1.10	542	37	533	11	531	11	98				
44WP103L_10-25-50	25	69	34	0.18723	0.82	13.12967	1.23	0.50861	0.92	2718	27	2689	23	2651	40	98				
45WP103L_10-50-50	50	204	8	0.05305	0.84	0.35069	1.34	0.04795	1.05	331	38	305	7	302	6	91				
46bWP103L_10-35-50	35	155	57	0.13388	0.81	7.40759	1.31	0.40128	1.04	2150	28	2162	24	2175	38	101				
46WP103L_10-25-50	25	58	23	0.14550	0.85	8.52840	1.31	0.42511	1.00	2294	29	2289	24	2284	38	100				
47WP103L_10-50-50	50	57	29	0.18731	0.80	13.69790	1.24	0.53039	0.94	2719	26	2729	24	2743	43	101				
48WP103sm_10-35-50	35	65	37	0.21689	0.80	17.42037	1.22	0.58254	0.91	2958	26	2958	23	2959	43	100				
49WP103sm_10-35-50	35	209	116	0.20950	0.80	16.28272	1.26	0.56369	0.98	2902	26	2894	24	2882	46	99				
50WP103sm_10-35-50	35	117	67	0.21350	0.80	17.03627	1.28	0.57872	0.99	2932	26	2937	25	2944	47	100				
51WP103sm_10-35-50	35	390	200	0.18576	0.80	13.56395	1.31	0.52958	1.03	2705	26	2720	25	2740	47	101				
52WP103sm_10-35-50	35	197	110	0.21518	0.80	17.18238	1.46	0.57914	1.22	2945	26	2945	28	2945	58	100				
53WP103sm_10-35-50	35	135	43	0.12092	0.81	5.96534	1.29	0.35780	1.00	1970	29	1971	23	1972	34	100				
54WP103sm_10-50-50	50	17	9	0.20733	0.81	16.27294	1.37	0.56926	1.10	2885	26	2893	26	2905	52	101				